

# Constraining the provenance of the Stonehenge 'Altar Stone': evidence from automated mineralogy and U-Pb zircon age dating

Richard E. Bevins<sup>a,b</sup>, Duncan Pirrie<sup>c</sup>, Rob A. Ixer<sup>d</sup>, Hugh O'Brien<sup>e</sup>, Mike Parker Pearson<sup>d</sup>, Matthew R. Power<sup>f</sup>, Robin K. Shail<sup>g</sup>

<sup>a</sup>*Department of Natural Sciences, National Museum of Wales, Cathays Park, Cardiff CF10 3NP, UK*

<sup>b</sup>*Department of Geography and Earth Sciences, Aberystwyth University, Aberystwyth SY23 3DB, UK*

<sup>c</sup>*School of Applied Sciences, University of South Wales, Pontypridd CF37 4BD, UK*

<sup>d</sup>*Institute of Archaeology, University College London, London WC1H 0PY, UK*

<sup>e</sup>*Geological Survey of Finland (GTK), Betonimiehenkuja 4 02150, Espoo, Finland*

<sup>f</sup>*Vidence Inc., Suite #259, 4111 Hastings Street, Burnaby, British Columbia, V5C 6T7, Canada*

<sup>g</sup>*Camborne School of Mines, College of Engineering, Mathematics and Physical Sciences, University of Exeter, Cornwall Campus, Penryn, Cornwall TR10 9FE UK*

Keywords: Stonehenge, Bluestones, Altar Stone, sandstone, provenancing, automated mineralogy, U-Pb age dating

Declaration of competing interests: none

## Abstract

The Altar Stone at Stonehenge is a greenish sandstone thought to be of Late Silurian-Devonian ('Old Red Sandstone') age. It is classed as one of the bluestone lithologies which are considered to be exotic to the Salisbury Plain environ, contrasting with the larger sarsen stones, which are a hard, durable silcrete derived from no more than 30km from Stonehenge. It is well established that most of the bluestones are derived from the Mynydd Preseli, in west Wales. However, no Old Red Sandstone rocks crop out in the Preseli; instead a source in the Lower Old Red Sandstone Cosheston Subgroup at Mill Bay, on the shores of Milford Haven, to the south of the Preseli, has been proposed. More recently, on the basis of detailed petrography, a source for the Altar Stone much further to the east, towards the Wales-England border, has been suggested. Quantitative analyses presented here compare data from proposed

Stonehenge Altar Stone debris with samples from the Cosheston Subgroup at Mill Bay in west Wales, as well as with a second sandstone type found at Stonehenge which, on palaeontological evidence has been shown to be Lower Palaeozoic in age. The Altar Stone samples have up to 16.7 modal % calcite while the Lower Palaeozoic and Cosheston Subgroup sandstones have less than 0.25 modal %. The Altar Stone also contains up to 3.8 modal % kaolinite and 0.8 modal % barite, minerals that are absent from the other sandstones. Calcite, kaolinite and barite in the Altar Stone samples all occur between the detrital grains and are all thought to be authigenic minerals, which differs markedly with the Cosheston Subgroup and Lower Palaeozoic sandstones. The Cosheston Subgroup sandstone contrasts with the other two sandstone lithologies in having up to 0.7 modal % detrital garnet (<0.08 in both the other two sandstone types). Further differences between the Altar Stone sandstone and the Cosheston Subgroup sandstone are seen when their contained zircons are examined. Not only do they have differing morphologies (size, shape and quality) but U-Pb age dates for the zircons show contrasting populations; the Cosheston Subgroup sample zircon age population is essentially bimodal, with age maxima at 500 and 1500 Ma whilst the Altar Stone zircon population is more diverse, with ages spanning from 472 to 2475 Ma without maxima. Together, all these data confirm that Mill Bay is not the source of the Altar Stone with the abundance of kaolinite in the Altar Stone sample suggesting a source further east than Milford Haven, towards the Wales-England border. The disassociation of the Altar Stone and Milford Haven fully undermines the hypothesis that the bluestones, including the Altar Stone, were transported from west Wales by sea up the Bristol Channel and adds further credence to a totally land-based route, possibly along a natural routeway leading from west Wales to the Severn estuary and beyond. This route, along the valleys followed today by the A40, may well have been significant in prehistory, raising the possibility that the Altar Stone was added *en route* to the assemblage of Preseli bluestones taken to Stonehenge around or shortly before 3000 BC. Recent strontium isotope analysis of human and animal bones from Stonehenge, dating to the beginning of its first construction stage around 3000 BC, are consistent with having lived in this western region of Britain.

This study appears to be the first application of quantitative automated mineralogy in the provenancing of archaeological lithic material and highlights the potential value of automated mineralogy in archaeological provenancing investigations, especially when combined with complementary techniques, in the present case U-Pb age dating of zircons.

## **1. Introduction**

For much of the 20<sup>th</sup> century provenancing studies of archaeological lithics were based largely on hand specimen or standard transmitted light petrographical investigations, the latter chiefly focussing on the most abundant rock-forming minerals but sometimes also assessing accessory or heavy minerals. It was largely qualitative with modal mineralogical analyses undertaken by manual point counting, a slow, laborious task with the potential for considerable error (for example by Ixer and Turner, 2006).

With the advent of a wide range of analytical geochemical and mineralogical techniques (e.g. whole rock X-ray fluorescence spectroscopy, instrumental neutron activation analysis, stable isotope analysis, radiometric dating, X-ray diffraction, scanning electron microscopy with energy dispersive analysis, electron micro-probe analysis and, more recently, inductively coupled plasma-mass spectrometry and portable XRF; Hunt (2016)) and their routine use in petrological studies, it has become possible to apply the same methodologies to both natural and man-made archaeological materials.

In this paper we combine mineralogical characterisation using automated scanning electron microscopy (Pirrie and Rollinson, 2011) with zircon age dating to test the source of stone 80, the 'Altar stone', from Stonehenge. This is a greenish sandstone thought to be of Late Silurian-Devonian age ('Old Red Sandstone') and considered to be one of the Stonehenge bluestone lithologies (see Cleal et al., 1995). Understanding the provenance of the Altar Stone is of considerable importance. H.H. Thomas, who in 1923 provided the first modern descriptions and provenancing of the bluestones (see below), proposed that the pale sage-green micaceous sandstone

had a strong similarity to either sandstones from the Senni Formation, cropping out between Kidwelly and Abergavenny in south Wales or to sandstones from the Cosheston Subgroup (lateral equivalent of the Senni Formation) from the shore of Milford Haven in west Wales (Fig. 1). This suggested Milford Haven source area profoundly influenced thinking as to how the bluestones were transported to Stonehenge, in particular the notion of transport of the stones by sea, at least for a large part of the journey, which became firmly established in the secondary literature for example by Atkinson (1956) and Darvill (2006) (but see Parker Pearson et al., 2015b for a more recent perspective). However, results of detailed petrographic examinations of the Altar Stone sandstone and sandstones from Old Red Sandstone outcrops in west Wales have called into question the Cosheston Subgroup source for the Altar Stone (see Ixer et al., 2020 for a thorough review) and the notion of the bluestones being put onto rafts at Milford Haven and transported up the Bristol Channel, before a final land route across to Salisbury Plain. The recent proposal that Craig Rhos-y-felin and Carn Goedog on the northern flanks of the Mynydd Preseli represent sites of Neolithic quarrying for Stonehenge bluestone (Parker Pearson et al., 2015a, 2019) raises further doubts for any logical rationale for a southerly transport route up and over the Preseli Hills and down to Milford Haven. Having said that, there are still some who doubt that the bluestones were transported by humans, arguing instead for transport by ice (John et al., 2015).

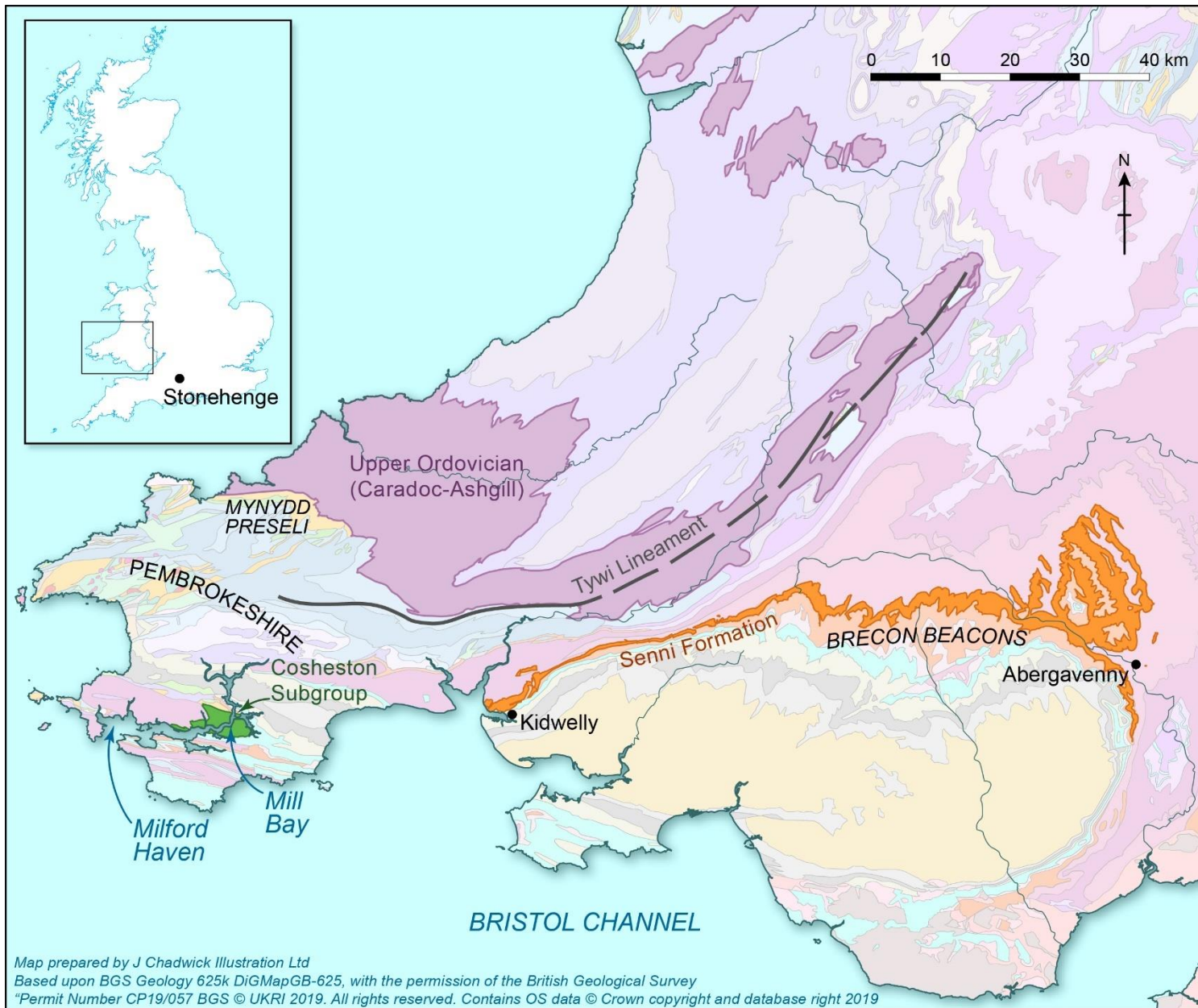


Fig. 1. Map of southern Wales showing the distribution of the Cosheston Subgroup and the Senni Formation of Late Silurian to Devonian age (belonging to the 'Old Red Sandstone'). Also shown (in purple) is the extent of Upper Ordovician (Caradoc-Ashgill) strata in southern Wales lying to the east and northeast of the Mynydd Preseli. Geological details based upon British Geological Survey Geology 625kDiGMapGB-625 and the line of the Tywi Lineament is from Earthwise. With permission Permit Number 19/057 BGS © UKRI 2019. All rights reserved. Contains OS data Crown © and database right 2019.

Here we apply quantitative mineralogical and geochemical approaches to robustly test whether the Cosheston Subgroup at Milford Haven could have been the source of the Stonehenge Altar Stone or indeed any other bluestone sandstones found at Stonehenge, as has recently been challenged on the basis of detailed petrographic investigations (Ixer et al., 2019, 2020). If this can be disproved, then it adds further scientific support to challenge the proposed marine transport route for the bluestones.

Finally, this paper represents the first time that automated mineralogy has been used in archaeological provenancing investigations and highlights its potential, especially when used in combination with a complimentary analytical technique, in this case U-Pb dating of zircons.

## **2. Stonehenge bluestone provenancing studies**

The various rock types used in the construction of Stonehenge have long been recognised as being of two types, namely the sarsens, the large silcrete stones thought to be derived relatively locally from the Stonehenge environ (see Parker Pearson, 2016), and the bluestones, a generic term for rock types exotic to the Stonehenge area and for nearly a century thought to be derived from sources in west Wales (Thomas, 1923). The bluestones comprise a range of lithologies, namely dolerite, rhyolite, volcanic tuff and two types of sandstone, one being of Lower Palaeozoic age on the basis of contained acritarch fossils, the second being the so-called Altar

Stone which is thought to be derived from the Late Silurian-Devonian Old Red Sandstone. The Altar Stone, stone 80, is the focus of this paper.

Since 2010, there has been an on-going extensive review of the petrography of the bluestones (Ixer and Bevins, 2010, 2011a,b, 2013, 2016; Ixer et al., 2015, 2017, 2019, 2020). Petrographic data have been combined with new geochemical data which has included laser ablation ICP-MS zircon chemistry (Bevins et al., 2011), a re-interpretation of whole rock XRF data for the dacites/rhyolites and the dolerites (Bevins et al., 2012, 2014) and application of U-Pb zircon radiometric dating of rhyolitic debris at Stonehenge and from the Mynydd Preseli in west Wales (Bevins et al., 2017). Results from these studies have called into question many of the original sources proposed by Thomas (1923) and later proposals by Thorpe et al. (1991), as discussed in Bevins et al. (2014) and Bevins and Ixer (2018).

As a result of these studies the origins of the two types of sandstone present within the bluestone assemblage have also been reconsidered (see Ixer et al., 2020). As mentioned above, one type of sandstone is present as debris in the Stonehenge Landscape but also probably forms the concealed stones numbered 40g and 42c. This lithology is thought to be of Lower Palaeozoic age on the basis of its contained acritarch assemblages and is probably derived from the ground to the northeast and east of the Preseli but west of the Tywi Lineament (see Fig. 1) (Ixer et al., 2017). The second type of sandstone, found as rare debris at Stonehenge as well as comprising the Altar Stone (stone 80), is also not derived from the Mynydd Preseli area.

Although preliminary automated SEM-EDS mineralogy data for the Altar Stone were described and briefly discussed by Ixer et al. (2020), in this paper the automated mineralogy (SEM-EDS) data are presented in full, including new analyses of a further three debris samples, also thought to be derived from the Altar Stone. We combine evidence from this approach with U-Pb radiometric data obtained from zircons from an Altar Stone sample and a Lower Old Red Sandstone sample from the Coshaston Subgroup at Mill Bay, Milford Haven. For completeness we analysed the Lower Palaeozoic Sandstone lithology using automated mineralogy in order to highlight mineralogical differences to the Altar Stone. Finally we (1) review the potential value of automated mineralogy in

archaeological provenancing investigations, (2) discuss the implications of the results of these investigations on the possible origin of the Altar Stone, (3) identify what approaches might be pursued to refine further the possible source area of the Altar Stone, and (4) briefly consider what our findings show in terms of the broader significance of the bluestones, their potential sources and the means of transport of the stones to Stonehenge.

### **3. Methodology and samples studied**

#### *3.1. Automated Mineralogy*

Automated SEM-EDS provides fully quantitative data on mineral abundances. The method is also effective to visualise mineralogical assemblages and associations. The method has therefore proven especially useful in diagenetic and sedimentological studies (e.g. Armitage et al., 2010; Carter et al., 2017) where the textural association of the minerals is of key importance. In addition, the technique has previously been applied in a range of archaeological investigations including the analysis and provenancing of ceramics (e.g. Knappett et al., 2011; Hilditch et al., 2016), the composition of ancient Egyptian cosmetics (e.g. Hardy et al., 2006), and in the provenancing of archaeological artefacts using soil forensics (Pirrie et al., 2014).

In this study, the samples were analysed using a FEI Quanta 650 QEMSCAN system operating at 20 kV and a measured beam current of 10 nA. Data were collected at a 10 µm stepping interval which resulted in the collection of between 1,222,274 and 3,474,526 individual EDS analysis points per sample. Raw data were processed using iDiscover 5.4 software and reported numerically as modal mineralogy % and graphically as false colour images where each identified mineral phase is assigned to a colour. Details of this analytical method are summarised in Pirrie et al. (2004) and Pirrie and Rollinson (2011).

With automated mineralogy it can be possible to assign particles to lithological groupings based on mineralogy, texture and grain/crystal size (lithotyping; see Pirrie et al., 2013). However, in this study the automated SEM-EDS mineralogical data are only



reported as modal % which means that fine-grained lithic fragments, which can comprise up to 3.5% of the grains in the Lower Palaeozoic Sandstone lithology (data from Thomas in Thorpe et al., 1991), are not individually recognised and are instead reported in the data as their constituent minerals. Similarly, in sediment provenance studies, different textural varieties of quartz (e.g. monocrystalline vs polycrystalline quartz, quartz showing straight extinction vs quartz showing undulose extinction etc.) can be significant in terms of determining the source area geology. However, as mineral identification by automated mineralogy is based on chemistry, these textural types are not automatically identified. Conversely, the identification of a range of minerals can prove challenging using optical methods and as such may be mis-reported during polarising light microscopy. For instance, small grains of plagioclase or alkali feldspar may lack characteristic optical features such as twinning and hence untwinned plagioclase were recorded as alkali feldspar by Ixer and Turner (2006). Data here are reported to two decimal places to highlight key mineralogical differences in phases which occur at low abundance.

In total, twelve sandstones were analysed by automated SEM-EDS for this investigation (see Table 1). Of these, nine are Stonehenge Landscape sandstone debitage, six of which have been identified petrographically as being derived from the Altar Stone (Ixer and Bevins, 2013; Ixer et al., 2020) and three of which, based on petrographic characteristics and acritarch evidence (Ixer et al., 2017), have been identified as being of Lower Palaeozoic age. The remaining three samples were collected from the previously proposed Altar Stone source lithologies of the Cosheston Subgroup that crop out at Mill Bay and at nearby Whalecwm, both localities on the shores of Milford Haven (Ixer et al., 2020). Modal mineralogical data are presented in Table 2 and in Fig. 2.

Sample number	Lithological grouping	Description
FN573	Altar Stone	SH08 Context 16 FN573 (previously erroneously labelled as FN593). From a Roman context at Stonehenge. Described in Ixer and Bevins (2013).

HM13	Altar Stone	From Context 3 spit V/1 from the Stonehenge Layer excavated in May 2008 (Darvill and Wainwright, 2009). Described in Ixer and Bevins (2013).
SH 08	Altar Stone	SH08 Context 1 FN196. From modern overburden at Stonehenge. Described in Ixer and Bevins (2013).
MS-1	Altar Stone	Excavated by Hawley from close to stone 1. Described in Ixer et al. (2019). Salisbury Museum Collection.
MS-2	Altar Stone	Excavated by Hawley from close to stone 1. Described in Ixer et al. (2019). Salisbury Museum Collection.
MS-3	Altar Stone	Excavated by Hawley from close to stone 1. Described in Ixer et al. (2019). Salisbury Museum Collection.
1 Cursus	Lower Palaeozoic Sandstone	Cursus (From sample 1947/142.18 and also the source of SASII thin section 275). Excavated by Stone in 1947 at the Cursus Ditch. Described in Ixer et al. (2017).
OU9	Lower Palaeozoic Sandstone	OU9 (Salisbury Museum sample 444). Excavated by Hawley from Aubrey Hole 1. Labelled 'Hawley 444 Cosheston Beds?'. Described by Thomas (1991, 152-153) and by Ixer and Turner (2006, 8).
656A	Lower Palaeozoic Sandstone	656A (SH79). Section made from rock number 656 (79 FN656 L/2 27.5.79). Excavated by Pitts and mentioned by Howard (in Pitts, 1982). Described in detail in Ixer et al. (2017).
Mill Bay 1a	Cosheston Subgroup	Mill Bay 1a. Sample collected from Mill Bay by Brian John.
Mill Bay 1b	Cosheston Subgroup	Mill Bay 1a. Sample collected from Mill Bay by Brian John.
Mill Bay 3	Cosheston Subgroup	Mill Bay 3. Sample collected from Whalecwm by Brian John.

Table 1. Details of samples analysed in this study.

Sample Name	FN 573	HM 13	SH 08	MS-1	MS-2	MS-3	Mill Bay 1a	Mill Bay 1b	Mill Bay 3	1 (cursus ditch)	OU9	656A (SH79)
Source	Altar Stone	Altar Stone	Altar Stone	Altar Stone	Altar Stone	Altar Stone	Cosheston Subgroup	Cosheston Subgroup	Cosheston Subgroup	Lower Palaeozoic Sandstone	Lower Palaeozoic Sandstone	Lower Palaeozoic Sandstone
Quartz	55.96	55.00	54.91	55.34	55.40	53.64	54.17	54.30	55.11	68.13	69.14	69.99
K feldspar	0.21	0.23	0.25	0.24	0.24	0.23	0.35	0.37	0.61	0.04	0.03	0.03
Plagioclase	12.11	12.59	12.24	12.18	12.14	12.00	23.22	23.20	22.45	12.81	13.96	14.11
Muscovite	2.12	2.62	2.51	2.57	2.49	2.54	5.02	4.74	5.73	5.51	3.59	3.87
Biotite	0.45	0.51	0.55	0.58	0.48	0.50	0.99	0.98	1.21	0.15	0.10	0.13
Kaolinite	3.05	3.16	3.26	3.21	3.22	3.79	0.15	0.15	0.10	0.09	0.11	0.08
Chlorite	4.37	5.15	5.11	4.44	4.36	4.28	6.02	6.27	4.74	5.36	5.13	5.36
Illite & illite-smectite	4.25	5.19	4.83	3.82	3.78	3.86	5.13	5.31	5.22	5.64	3.97	4.35
Fe-Illite & illite-smectite	0.91	1.08	1.18	0.93	0.80	0.73	3.22	3.17	3.85	1.47	0.93	1.31
Calcite	14.41	12.58	13.68	14.71	14.98	16.63	0.03	0.03	0.02	0.02	0.25	0.03
Dolomite	0.60	0.59	0.61	0.45	0.47	0.46	0.00	0.01	0.00	0.00	0.72	0.00
Ferroan dolomite	0.02	0.02	0.02	0.02	0.02	0.02	0.00	0.00	0.00	0.00	1.29	0.00
Fe oxides	0.00	0.01	0.00	0.01	0.01	0.01	0.05	0.03	0.27	0.04	0.05	0.06
Chromite	0.03	0.02	0.01	0.01	0.02	0.02	0.01	0.01	0.00	0.00	0.00	0.00
Pyrite	0.01	0.01	0.01	0.01	0.00	0.00	0.03	0.00	0.02	0.00	0.03	0.00
Barite	0.67	0.54	0.29	0.75	0.80	0.59	0.01	0.01	0.00	0.00	0.00	0.00

Anhydrite	0.00	0.00	0.00	0.00	0.00	0.00	0.00	0.00	0.00	0.00	0.00	0.00
Halite	0.00	0.00	0.00	0.01	0.00	0.00	0.03	0.05	0.01	0.00	0.00	0.00
Rutile & Ti Silicates	0.38	0.33	0.25	0.32	0.36	0.31	0.57	0.53	0.29	0.33	0.28	0.29
Ilmenite	0.03	0.02	0.01	0.03	0.05	0.04	0.01	0.01	0.00	0.00	0.00	0.00
Apatite	0.25	0.18	0.14	0.21	0.20	0.20	0.14	0.15	0.03	0.25	0.24	0.24
Garnet	0.08	0.07	0.07	0.06	0.07	0.06	0.72	0.59	0.30	0.05	0.08	0.06
Tourmaline	0.04	0.06	0.05	0.06	0.06	0.06	0.03	0.03	0.03	0.03	0.02	0.03
Zircon	0.04	0.04	0.02	0.04	0.05	0.03	0.08	0.06	0.01	0.06	0.04	0.04

Table 2. Modal mineralogy of samples analysed in this study from the Stonehenge Altar Stone, the Cosheston Subgroup in Pembrokeshire and from Lower Palaeozoic Sandstone debris samples from various contexts at Stonehenge (see Table 1 for sample details).

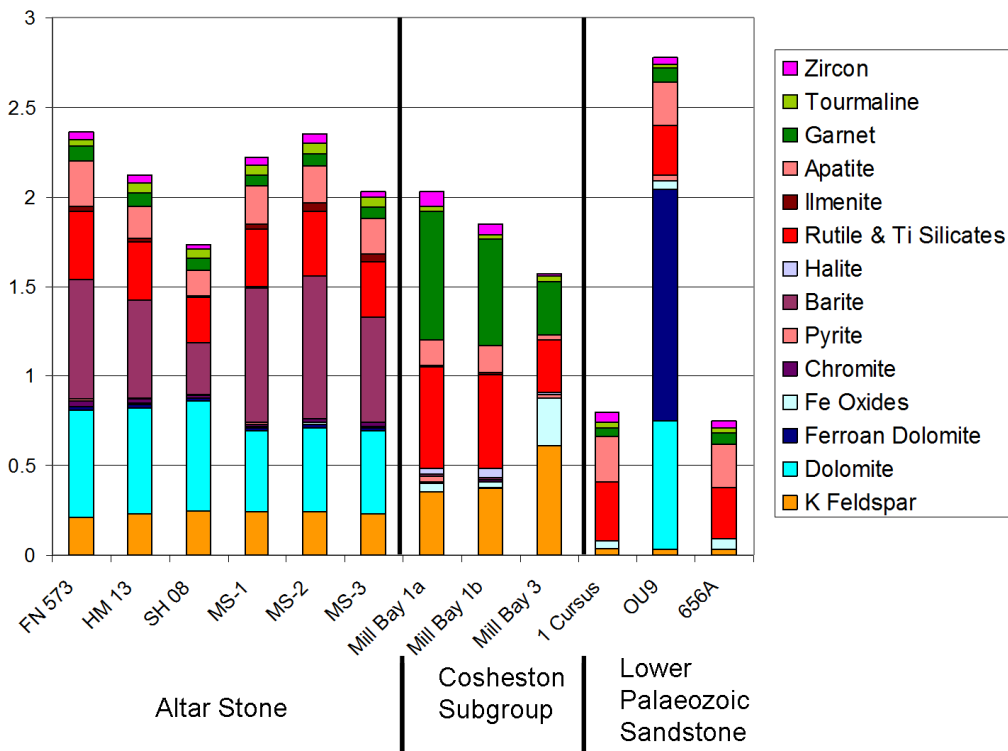
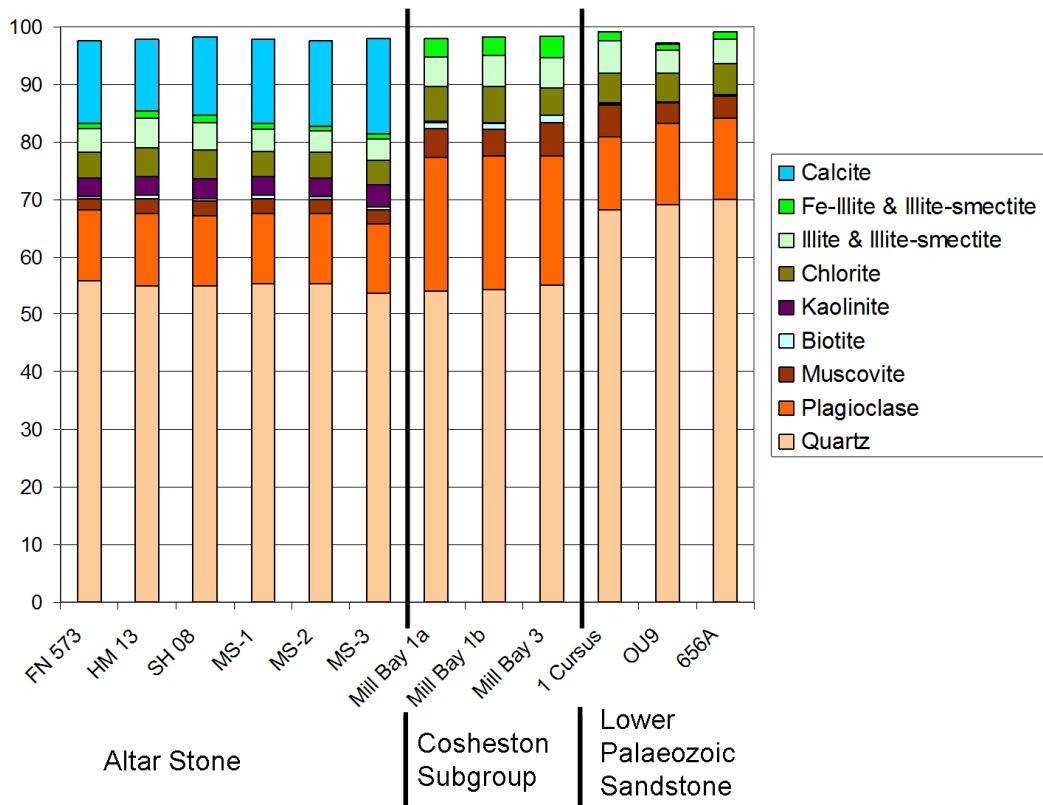


Fig. 2. Modal mineralogy histograms for samples from the Stonehenge Altar Stone (FN573, HM13, SH 08, MS-1, MS-2, MS-3), the Cosheston Subgroup (Mill Bay 1a, Mill Bay 1b, Mill Bay 3) at Mill Bay in Pembrokeshire and Lower Palaeozoic bluestone sandstone debris from various contexts at Stonehenge (1 Cursus, OU9, 656A). Upper: Minerals with a modal abundance >1%. Lower: Minerals with a modal abundance <1%.

### *3.2. Radiometric dating*

Zircon grains for U-Pb dating were selected by an automated SEM search for high mass features in two polished thin sections, one from the Altar Stone (sample FN573) and one from exposures of the Cosheston Subgroup (Old Red Sandstone) at Mill Bay, in west Wales (sample Mill Bay 1a). Following the automated scan, operator controlled back-scattered electron imaging of the largest zircon grains was undertaken to provide a record of each grain to be analysed prior to ablation by the laser and to assist with targeting the spot analysis sites. Coordinates of the target grains recorded from the SEM were re-coordinated in the laser ablation system using transmission electron microscopy reference grids. Feature numbers allow tracking of each grain's backscatter electron (BSE) image and U-Pb data.

U-Pb dating analyses were performed using a Nu Plasma AttoM single collector ICPMS at the Geological Survey of Finland in Espoo connected to a Photon Machine Excite laser ablation system. Samples were ablated in He gas (gas flows = 0.4 and 0.1 l/min) within a HelEx ablation cell (Müller et al., 2009). The He aerosol was mixed with Ar (gas flow= 0.8 l/min) prior to entry into the plasma and the gas mixture was optimized daily for maximum sensitivity. Typical ablation conditions were: beam diameter 25µm; pulse frequency 5Hz; and beam energy density 2 J/cm<sup>2</sup>. A single U-Pb measurement included a short pre-ablation, 10s of on-mass background measurement, followed by 30s of ablation with a stationary beam. <sup>235</sup>U was calculated from the signal at mass 238 using a natural <sup>238</sup>U/<sup>235</sup>U=137.88. Mass number 204 was used as a monitor for common <sup>204</sup>Pb. In an ICPMS analysis, <sup>204</sup>Hg mainly originates from the He supply. The observed background counting-rate on mass 204 was 150-200 cps (counts per second) during the period of the measurements. The contribution of <sup>204</sup>Hg from the plasma was eliminated by on-mass background measurement prior to each analysis. Age related common lead (Stacey and Kramers,

1975) correction was used when the analysis showed common lead contents significantly above the detection limit (i.e. >50 cps). Signal strengths on mass 206 were typically 100,000 cps, depending on the uranium content and age of the zircon.

Calibration standard GJ-1 ( $601.9 \pm 0.4$  Ma  $^{238}\text{U}/^{206}\text{Pb}$  age; Horstwood et al., 2016) and in-house standards A382 ( $1877 \pm 2$  Ma) and A1772 ( $2711 \pm 3$  Ma) ( $^{207}\text{Pb}/^{206}\text{Pb}$  ages; Huhma et al., 2012) were run at the beginning and end of each analytical session, and at regular intervals during sessions. Raw data were corrected for the background, laser induced elemental fractionation, mass discrimination and drift in ion counter gains and reduced to U-Pb isotope ratios by calibration to concordant reference zircons, using the program Glitter (Van Achterbergh et al., 2001). Further data reduction including common lead correction and error propagation was performed using an excel spreadsheet written by Y. Lahaye and H. O'Brien. Errors were propagated by quadratic addition of within-run errors (2 SE), the reproducibility of standard during the run (2 SD) and the overall error on the certification of the GJ-1 standard. To minimize the effects of laser-induced elemental fractionation, the depth-to-diameter ratio of the ablation pit was kept low, and isotopically homogeneous segments of the time-resolved traces were calibrated against the corresponding time interval for each mass in the reference zircon. Plotting of the U-Pb isotopic data and age calculations were performed using the Isoplot/Ex 3 program (Ludwig, 2003). All the ages were calculated with  $2\sigma$  errors and without decay constants errors. Data-point error ellipses are at the  $2\sigma$  level.

## **4. Results and interpretation**

### *4.1. Automated SEM-EDS*

#### *4.1.1. Modal mineralogy*

The modal mineralogy of the twelve sandstones presented in Table 2 shows that the samples fall into three distinct groups, each with a characteristic and tightly defined mineral assemblage. For instance, the six Stonehenge sandstones which have been identified on the basis of petrographic studies (Ixer and Bevins, 2013; Ixer et al., 2020) as being Altar Stone fragments and which come from various contexts at Stonehenge (see Table 1) are remarkably consistent in

terms of their modal mineralogy (Table 2, Fig. 2). These samples are dominated by quartz (53.64-55.96%), plagioclase (12.00-12.59%) and calcite (12.58-16.63%), the latter reflecting the carbonate cement which is considered a characteristic feature of the Altar Stone (Ixer et al., 2020). Other phases present in lesser quantities but of significance include kaolinite (3.05-3.79%), which is rare to absent in all other samples, muscovite (2.12-2.62%), biotite (0.45-0.58%), chlorite (4.28-5.15%), non-ferroan dolomite (0.45-0.61%), and illitic clays (including both illite & illite-smectite and Fe-illite and illite-smectite (4.58-6.27%). In addition, all of the Altar Stone samples contain small but notable amounts of barite (0.29-0.80%), K feldspar (0.21-0.25%) and ilmenite (0.03-0.05%). Hence, in addition to calcite, the presence of barite and kaolinite are defining characteristics of the Altar Stone although neither phase was recognised by Ixer and Turner (2006) using standard optical modal determinations of sample Wilts 277 (a Stonehenge debitage sample thought to be derived from the Altar Stone but unfortunately not re-analysed in this study because of the quality of the thin section).

Data from the three Lower Palaeozoic Sandstone (LPS) samples are also tightly constrained and represent a mineralogically well-defined group that is distinct from the Altar Stone samples (Table 2, Fig. 2). Samples from the LPS have less than 0.25% calcite but more quartz (68.13-69.99%), muscovite (3.59-5.51%) and plagioclase (12.81-14.11%) than the Altar Stone samples (Table 2, Fig. 2). Both the chlorite (5.13-5.36%) and illitic clay content (4.90-7.11%) are broadly similar to the Altar Stone samples whereas biotite, K feldspar and kaolinite are much less common (0.10-0.15%). Neither barite nor ilmenite are recorded in any of the LPS samples. Notably, one LPS sample (OU9) contains dolomite and ferroan dolomite cements (2.01% total dolomite); these values are higher than in any of the Altar Stone samples and indeed higher than in either of the other two LPS samples. What is worth noting, of course, is that there two LPS buried stumps at Stonehenge (stones 40g and 42c) so perhaps these are represented by OU9 and by 656A and 1 Cursus respectively.

On the basis of the mineralogy, the samples from the Cosheston Subgroup also form a tightly constrained group. Two samples from Mill Bay (1a, 1b) are from the same rock sample and sample 3 is from a similar lithology that crops out at Whalecwm, 500m north of Mill Bay. This suite of samples comprises major amounts of quartz (54.17-55.11%) and plagioclase (22.45-



23.22%) along with significant quantities of illitic clays (8.35-9.07%), chlorite (5.13-5.22%) and muscovite (4.74-5.73%). A range of minor to trace phases are also present including biotite (0.98-1.21%), K feldspar (0.35-0.61%) and, most significantly, comparatively abundant garnet (0.30 to 0.72%); the latter is a defining characteristic of the Cosheston Subgroup sandstones (Strahan et al., 1914) but uncommon in any of the Altar Stone (<0.08%) or LPS samples (<0.08%). Furthermore, carbonates (calcite and dolomite both < 0.03%), kaolinite (< 0.15%), barite and ilmenite (both <0.01%) are rare or absent from the mineral assemblage recorded in the Cosheston Subgroup samples but are common in, or characteristic of the Altar Stone suite of samples.

Given the consistency of the modal mineralogy recorded, the three petrological groups of samples can be clearly distinguished from each other. Because the data do not allow lithic grains to be determined, traditional sandstone provenance ternary diagrams cannot be utilised; however, if the three most abundant phases (quartz, plagioclase, and calcite) are plotted instead, the data are clearly discriminated (Fig. 3). Hence, the samples within each group are likely to have a common source but the source and diagenetic history of the Altar Stone, Cosheston Subgroup and LPS samples are different.

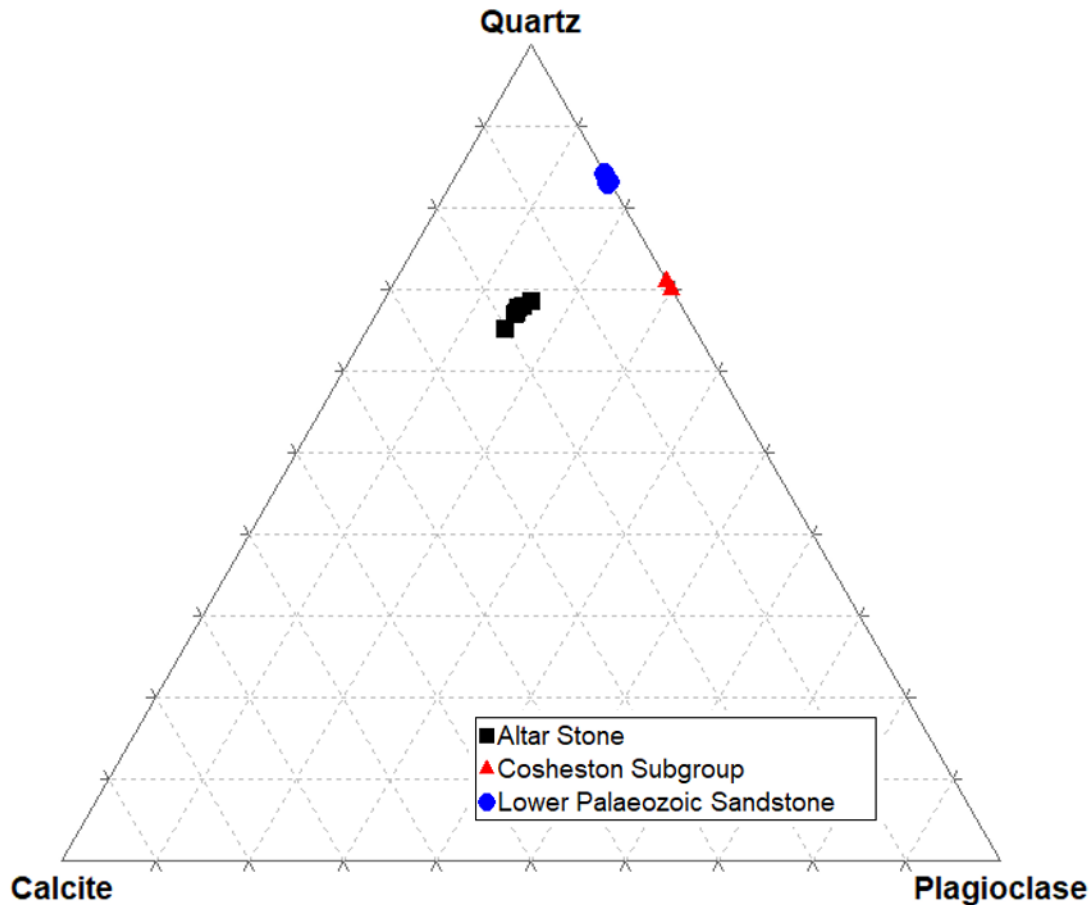


Fig. 3. Quartz-plagioclase-calcite ternary diagram for the analysed samples, showing clear discrimination of the three sandstone lithologies: Stonehenge Altar Stone, Cosheston Subgroup and the Lower Palaeozoic Sandstone bluestone debris from various contexts at Stonehenge.

#### 4.1.2. Mineralogical data in textural context

In addition to providing modal mineralogical data, automated SEM-EDS data are displayed as mineralogical maps of the imaged areas (Figs 4, 5). These images provide the mineralogical data in textural context and therefore can be “read” in the same way as a thin section photomicrograph, except in this case the interpreted mineralogical classifications are based on the chemical SEM-EDS analyses rather than optical properties. Textural context is important in terms of understanding the reported modal mineralogy, as mineral phases will either be detrital, diagenetic, or potentially metamorphic in origin. In the analysed samples the quartz, plagioclase and K feldspar (where present) occur primarily as a framework of discrete sand-grade grains

which are therefore interpreted to be detrital in origin and hence reflect the composition of the primary sediment source areas for the analysed lithologies. However, irregular and highly angular grain outlines are noted in several sections and particularly the LPS and Cosheston Subgroup samples which suggests that quartz and albite cementation, or grain boundary dissolution, may also have occurred.

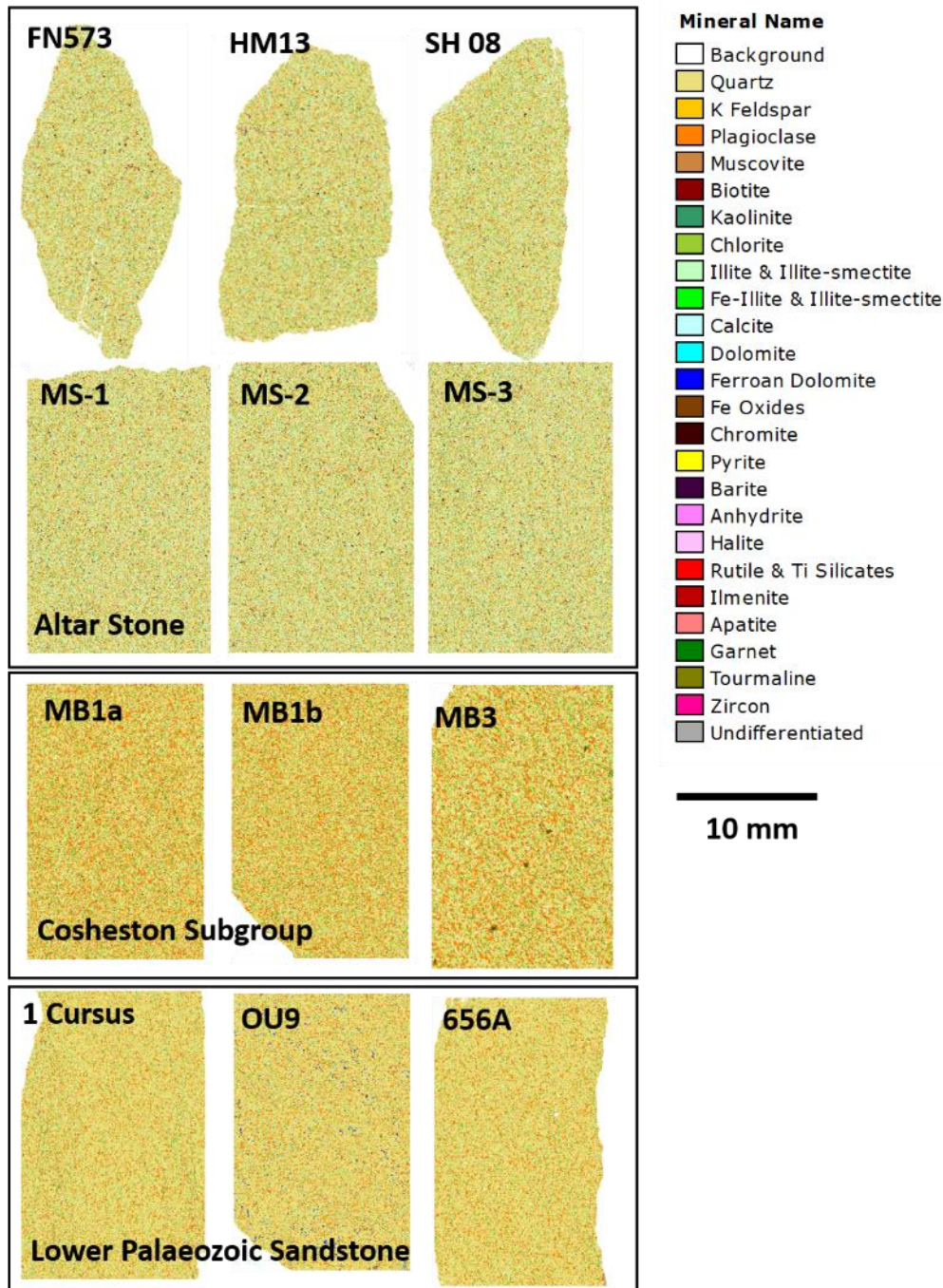


Fig. 4. False colour image particle maps generated by automated SEM-EDS for the samples analysed using a QEMSCAN system (see text for a description of the methodology). Samples FN573, HM13, SH 08, MS-1, MS-2 and MS-3 are from the Stonehenge Altar Stone, Mill Bay 1a, Mill Bay 1b and Mill Bay 3 are from the Cosheston Subgroup at Mill Bay in Pembrokeshire, and 1 Cursus, OU9 and 656A are debris samples of Lower Palaeozoic Sandstone from various contexts at Stonehenge.

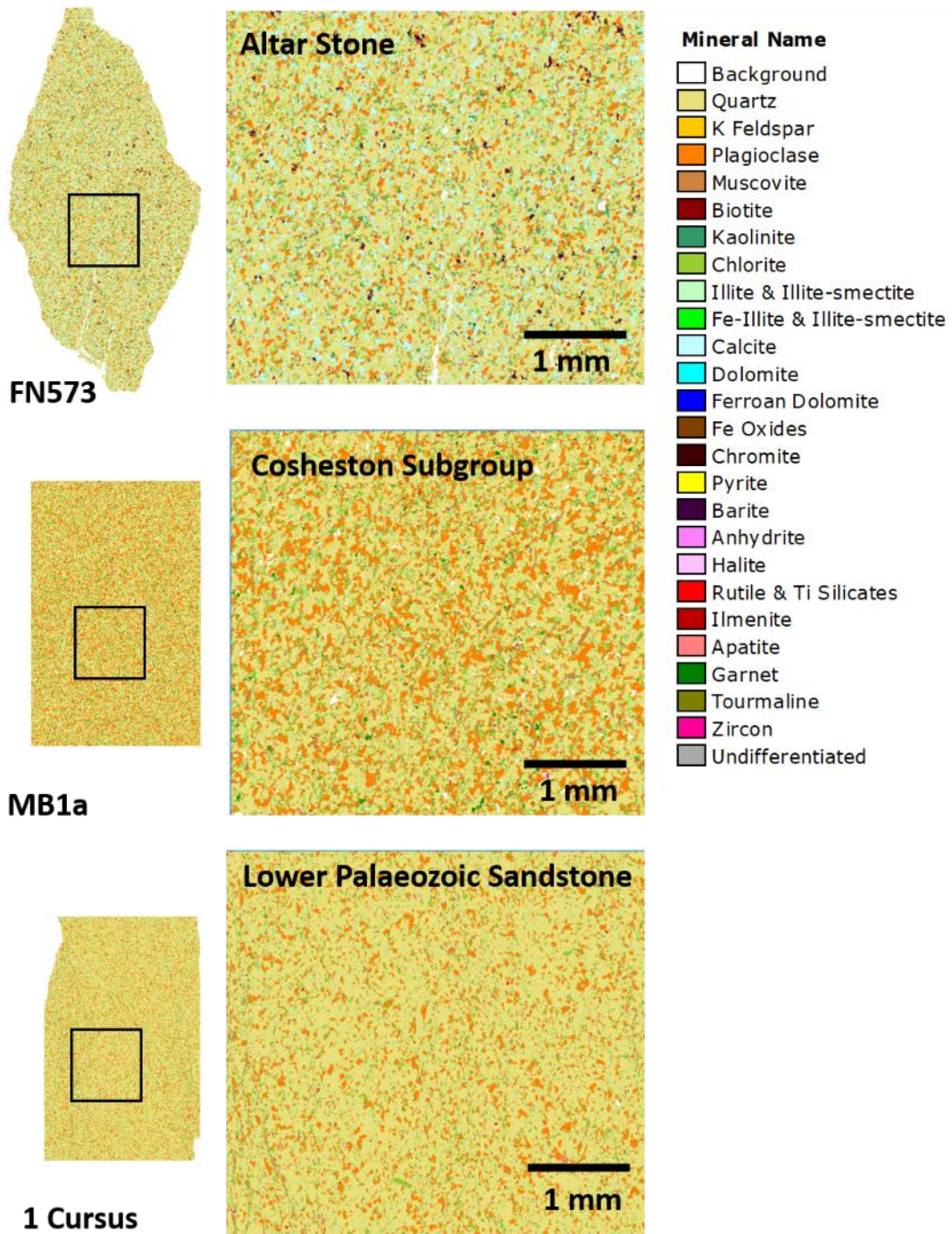


Fig. 5. Representative detailed false colour image particle maps for the three sandstone lithologies analysed by automated SEM-EDS. Clear mineralogical differences are readily visible between the three representative samples (see Fig. 4 caption for sample details).

The accessory or heavy minerals, Fe and FeTi oxides, chromite, rutile and Ti silicates, apatite, garnet, tourmaline and zircon all occur as scattered, small, often rounded grains that are interpreted as detrital in origin, although it should be noted that under specific diagenetic conditions, rutile and tourmaline can both occur as diagenetic phases. Fe oxides may be detrital but are more likely to be alteration/diagenetic phases after primary iron titanium oxides. Whilst combined the modal abundance of these phases is less than 1%, they can be very significant in terms of determining the original sediment source area.

Clay minerals in sandstones may occur as a detrital matrix or as either pore-lining or pore-filling diagenetic cements. A characteristic feature of the six samples analysed from the Altar Stone is the presence of abundant kaolinite which occurs as a pore-filling cement. Texturally this is interpreted as diagenetic kaolinite formed after the alteration/dissolution of plagioclase feldspar. When the samples interpreted as derived from the Altar Stone are compared with both the Lower Palaeozoic Sandstones and the samples from the Cosheston Subgroup, there is a significant reduction in kaolinite and an increased abundance of chlorite, illite and illite-smectite and Fe-illite and illite-smectite. This could either represent (a) variation in the original source area for detrital clay minerals, or (b) reflect different diagenetic/low grade metamorphic conditions. The illite and illite-smectite and Fe illite and illite-smectite are interpreted as diagenetic/low grade metamorphic in origin. Whilst muscovite is a relatively common detrital mineral, this compositional grouping would also include other white micas such as sericite, which may form as a diagenetic/low grade metamorphic mineral with, for example, sericitisation of feldspars. The biotite present is detrital in origin.

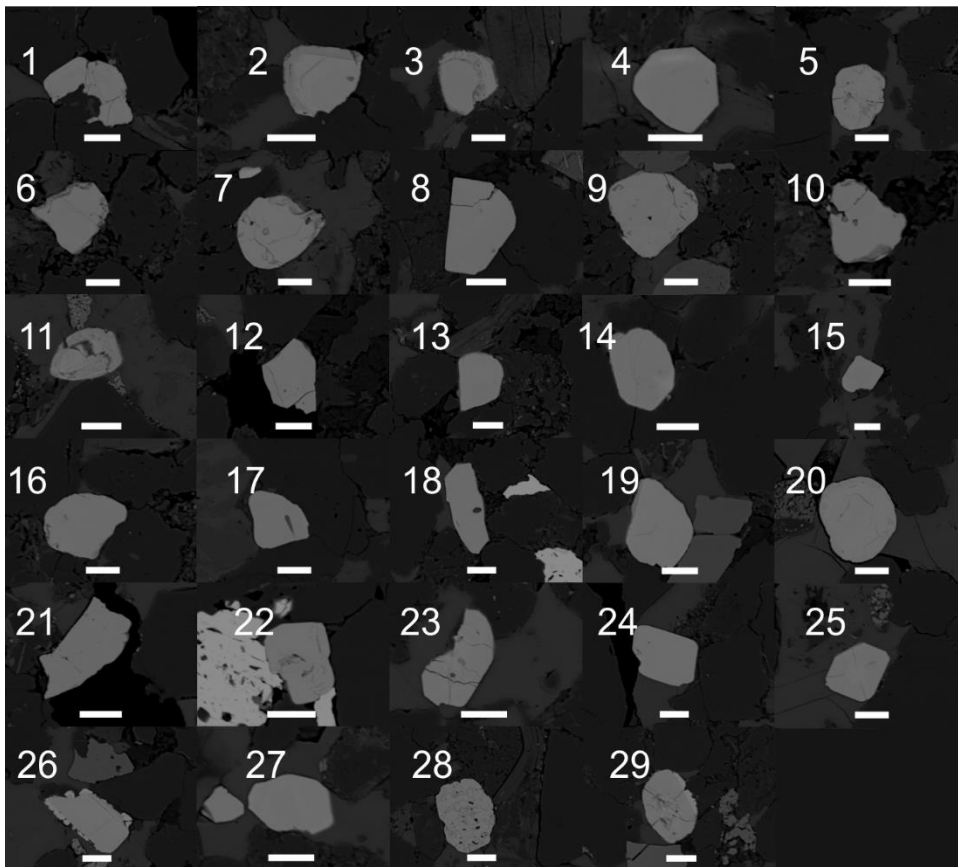
Carbonate minerals (calcite, dolomite and Fe dolomite) are present in the Altar Stone samples where they occur as an intergranular, pore-filling cement and are therefore interpreted to be diagenetic in origin. Texturally, the Altar Stone sandstone samples show that they are pervasively calcite cemented unlike either the analysed Lower Palaeozoic Sandstone or the Cosheston Subgroup samples. In addition, the detrital grains are moderately tightly packed, suggesting that calcite cementation occurred either during or following compaction (Fig. 5). The Lower Palaeozoic Sandstone samples split into two groups based on carbonate minerals; samples 1 (Cursus ditch) and 656A only contain trace calcite (0.02-0.03%) and no dolomite or ferroan

dolomite, whilst sample OU9 contains moderately abundant ferroan dolomite (1.29%) along with trace dolomite (0.72%) and calcite (0.25%). Barite also occurs as a rare mineral (0.29-0.80%) present within the Altar Stone samples, whilst being essentially absent in the LPS and Cosheston Subgroup samples. Given that the barite occurs between detrital grains it is also interpreted as diagenetic in origin. Pyrite is also present as a very minor diagenetic phase. The textural images for the three Altar Stone samples SH08, FN573 and HM13 are very similar, supporting the suggestion by Ixer et al. (2020) that they are all in fact from the same large block of rock. In turn, the differences between the Altar Stone samples and those from the Cosheston Subgroup and the Lower Palaeozoic Sandstone samples are readily observable.

## 5. Radiometric dating

The results of zircon imaging and radiometric dating for the two analysed samples, FN573 (Altar Stone fragment) and Cosheston Subgroup sample Mill Bay 1a, unequivocally show that the samples have distinct zircon populations based on four key observations listed in order of increasing merit. (1) Zircon grain size: The largest 30 grains in the Altar Stone sample are, on average, roughly half the size of the largest 30 grains from the Cosheston Subgroup sample (Fig. 6). (2) Zircon grain shape: Coupled with grain size, the grain shapes of the two populations are quite distinct. The Altar Stone grains are nearly all equidimensional, equant to rounded grains. In contrast, the Cosheston Subgroup grain shapes are considerably more variable, ranging from rounded to elongate, with a number appearing to be grain fragments. A simple interpretation is that the Altar Stone grains reflect a more mature sedimentary environment with rounded grain morphologies, whereas the Cosheston Subgroup sample is less mature. (3) Zircon quality: Also readily apparent from the zircon BSE collages (Fig. 6) is the difference in condition of the two zircon populations. Nearly all the Altar Stone grains are unzoned, unaltered grains with only minor metamict areas. In contrast, the Cosheston Subgroup sample zircons show more alteration, some with highly metamict zones, embayments potentially from dissolution, and inclusions. However, surprisingly, the amount of common Pb in the Cosheston Subgroup zircon grains is significantly lower (i.e., they uniformly have high  $^{206}\text{Pb}/^{204}\text{Pb}$ ), whereas many of the

seemingly more pristine Altar Stone grains have high common Pb, and hence are discordant (plot below Concordia, see data in Table 3 and the concordia plots in Fig. 7). A possible explanation is that the apparently cleaner Altar Stone grains have been considerably more affected by pore fluids with resulting migration of radiogenic Pb out of and introduction of common Pb into the crystal structure of many of these zircons. Precipitation of barite and pervasive calcite cement in the Altar Stone sample noted above may be indicative of this fluid flow through the rock, simultaneously adversely affecting the zircons it contains. (4). Zircon ages: The Cosheston Subgroup sample zircon age population is essentially bimodal, with age maxima at 500 and 1500 Ma (Fig. 8b). In contrast, the Altar Stone zircon population is more diverse, with ages spanning from 472 to 2475 Ma, showing no maxima (Fig. 8a). Many Altar Stone grains and a few Cosheston Subgroup grains did not give suitable U-Pb data for age dating due to significant contamination by common Pb (all grains with  $^{206}\text{Pb}/^{204}\text{Pb} < 1500$  are unusable) or by showing greater than 15% discordance. These grains are marked with an asterisk in Table 3 and are not included in the plots of Fig. 8.





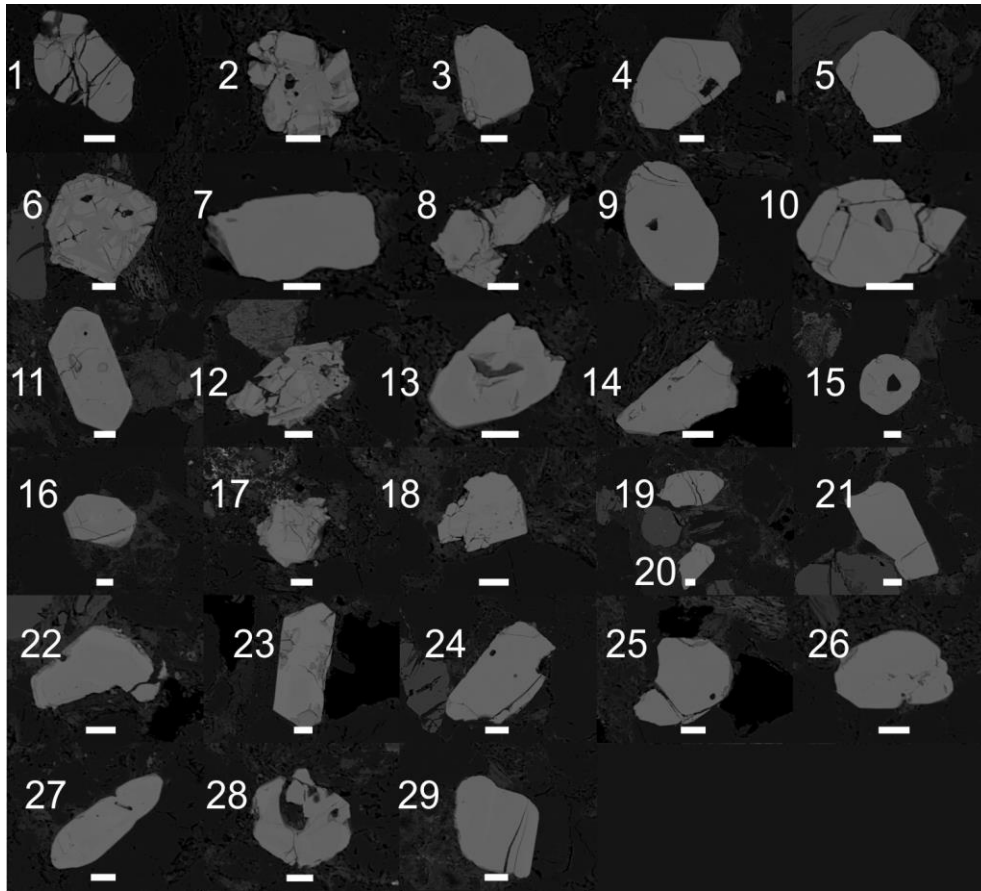


Fig. 6. Backscattered electron (BSE) images of the largest zircon grains from each thin section studied (a. upper is Altar Stone sample; b. lower is Cosheston Subgroup sample). Grains are labelled referring to corresponding analyses in Table 3. Scale bars are 20  $\mu\text{m}$ .

Table 3. U-Pb data for the zircon grains analysed from the Stonehenge Altar Stone and the Cosheston Subgroup Mill Bay samples

Figure 6

grain #	sample	$Pb^{206}/Pb^{204}$	$^{206}Pb_1$ (%)	Pb	Th	U	$^{207}Pb/^{206}Pb$	1s	$^{207}Pb/^{235}U$	1s	$^{206}Pb/^{238}U$	1s	r	% concordance	$^{207}Pb/^{206}Pb$	1s	$^{207}Pb/^{235}U$	1s	$^{206}Pb/^{238}U$	1s
1	Altar Stone-feature02*	286	6.0	137	188	411	0.1041	0.0004	3.437	0.104	0.240	0.007	0.99	82	1698	7	1513	23	1384	37
2	Altar Stone-feature05*	41	42.2	81	594	830	0.1479	0.0005	0.621	0.019	0.030	0.001	0.99	8	2322	6	490	12	193	6
3	Altar Stone-feature06	56660	0.0	26	30	60	0.1209	0.0005	5.908	0.178	0.355	0.011	0.99	99	1969	7	1962	26	1956	50
4	Altar Stone-feature10*	170	10.1	32	193	272	0.0481	0.0002	0.475	0.014	0.072	0.002	0.99	434	103	9	394	10	446	13
5	Altar Stone-feature11*	78	22.2	105	130	318	0.0925	0.0003	2.055	0.062	0.161	0.005	0.99	65	1477	7	1134	20	963	27
6	Altar Stone-feature13	19051	0.1	9	3	15	0.1605	0.0007	10.356	0.313	0.468	0.014	0.99	101	2461	8	2467	28	2475	61
7	Altar Stone-feature15*	195	8.8	91	155	366	0.0763	0.0003	1.761	0.053	0.167	0.005	0.99	91	1102	7	1031	19	998	28
8	Altar Stone-feature17	33934	0.1	15	83	164	0.0575	0.0003	0.619	0.019	0.078	0.002	0.99	95	510	11	489	12	485	14
9	Altar Stone-feature18	65366	0.0	27	19	106	0.0858	0.0003	2.737	0.083	0.231	0.007	0.99	101	1333	8	1338	22	1342	36
10	Altar Stone-feature19*	94	18.3	17	119	32	0.1019	0.0004	2.682	0.081	0.191	0.006	0.99	68	1659	8	1324	22	1126	31
11	Altar Stone-feature24*	119	14.4	54	192	513	0.1134	0.0006	0.839	0.025	0.054	0.002	0.99	18	1854	9	618	14	337	10
12	Altar Stone-feature26*	1630	1.1	60	85	221	0.1047	0.0004	3.244	0.098	0.225	0.007	0.99	76	1709	7	1468	23	1307	35
13	Altar Stone-feature27	3554	0.5	128	90	332	0.1092	0.0004	4.978	0.150	0.331	0.010	0.99	103	1786	7	1816	25	1842	48
14	Altar Stone-feature28*	42	41.4	140	218	209	0.1977	0.0007	5.931	0.179	0.218	0.007	0.99	45	2807	6	1966	26	1269	35
15	Altar Stone-feature30*	78	22.2	64	267	186	0.0834	0.0003	1.633	0.049	0.142	0.004	0.99	67	1280	7	983	19	856	24
16	Altar Stone-feature33	84871	0.0	42	83	91	0.1164	0.0005	5.628	0.170	0.351	0.011	0.99	102	1902	7	1920	26	1937	50
17	Altar Stone-feature39	14308	0.1	7	16	21	0.0981	0.0005	3.466	0.105	0.256	0.008	0.98	93	1588	10	1520	24	1471	39
18	Altar Stone-feature40	67478	0.0	30	193	336	0.0578	0.0002	0.605	0.018	0.076	0.002	0.99	90	523	9	481	11	472	14
19	Altar Stone-feature41*	706	2.4	58	151	198	0.0803	0.0003	2.410	0.073	0.218	0.007	0.99	106	1204	8	1246	21	1270	35
20	Altar Stone-feature42*	724	2.4	168	149	563	0.0852	0.0003	2.943	0.089	0.251	0.008	0.99	109	1319	8	1393	23	1442	39
21	Altar Stone-feature44*	2004	0.9	1	6	7	0.1098	0.0017	1.609	0.054	0.106	0.003	0.88	36	1796	28	974	21	651	19
22	Altar Stone-feature45*	620	2.8	126	309	560	0.0783	0.0003	1.877	0.057	0.174	0.005	0.99	90	1153	8	1073	20	1034	29
22	Altar Stone-feature45b*	58	29.6	65	121	253	0.1036	0.0004	1.489	0.045	0.104	0.003	0.99	38	1689	7	926	18	639	18
23	Altar Stone-feature46*	85	20.2	68	335	325	0.0695	0.0003	0.936	0.028	0.098	0.003	0.99	66	913	8	671	15	601	17
24	Altar Stone-feature47	86986	0.0	41	148	184	0.0742	0.0003	1.833	0.055	0.179	0.005	0.99	101	1048	8	1057	20	1062	29
25	Altar Stone-feature48*	240	7.2	37	270	224	0.0583	0.0002	0.809	0.024	0.101	0.003	0.99	114	541	9	602	14	618	18
26	Altar Stone-feature49*	1222	1.4	55	95	238	0.0770	0.0003	2.070	0.062	0.195	0.006	0.99	103	1120	8	1139	20	1149	32
27	Altar Stone-feature50	218049	0.0	91	79	406	0.0881	0.0003	2.514	0.076	0.207	0.006	0.99	87	1385	8	1276	22	1212	33
28	Altar Stone-feature51*	24	70.7	150	582	462	0.3832	0.0015	3.547	0.107	0.067	0.002	0.99	11	3845	6	1538	24	419	12
29	Altar Stone-feature52*	48	35.8	167	654	575	0.1257	0.0005	1.778	0.054	0.103	0.003	0.99	31	2038	7	1037	19	630	18

1	Millbay-feature06*	21736	0.1	12	139	102	0.0628	0.0003	0.703	0.021	0.081	0.002	0.98	72	703	11	541	13	503	15
2	Millbay-feature027*	154016	0.0	76	1119	1226	0.0592	0.0002	0.390	0.012	0.048	0.001	0.99	53	573	9	335	9	301	9
3	Millbay-feature031	15970	0.1	9	106	82	0.0555	0.0004	0.572	0.017	0.075	0.002	0.98	108	432	15	459	11	<b>465</b>	13
4	Millbay-feature045	108869	0.0	48	244	525	0.0566	0.0002	0.617	0.019	0.079	0.002	0.99	103	474	9	488	12	<b>491</b>	14
5	Millbay-feature058	8814	0.2	5	22	13	0.0941	0.0006	3.391	0.104	0.261	0.008	0.98	99	<b>1510</b>	13	1502	24	1497	40
6	Millbay-feature063	3556	0.5	97	564	1493	0.0536	0.0002	0.429	0.013	0.058	0.002	0.99	103	353	9	363	9	364	11
6	Millbay-feature063b*	126417	0.0	53	257	792	0.0586	0.0002	0.493	0.015	0.061	0.002	0.99	69	554	9	407	10	381	11
7	Millbay-feature073	97613	0.0	41	42	183	0.0771	0.0003	2.164	0.065	0.204	0.006	0.99	106	<b>1125</b>	8	1170	21	1194	33
10	Millbay-feature080	140232	0.0	60	79	219	0.0882	0.0003	2.976	0.090	0.245	0.007	0.99	102	<b>1386</b>	7	1401	23	1412	38
11	Millbay-feature081	102148	0.0	46	69	145	0.0961	0.0004	3.576	0.108	0.270	0.008	0.99	99	<b>1550</b>	7	1544	24	1540	41
12	Millbay-feature088*	30	57.5	4	14	3	0.3917	0.0024	19.522	0.594	0.361	0.011	0.98	51	3878	9	3068	29	1989	52
13	Millbay-feature097	16171	0.1	8	56	76	0.0572	0.0004	0.645	0.020	0.082	0.002	0.98	101	500	13	505	12	<b>506</b>	15
14	Millbay-feature110	40420	0.0	19	147	185	0.0569	0.0003	0.655	0.020	0.083	0.003	0.99	106	489	10	512	12	<b>517</b>	15
15	Millbay-feature117	29015	0.1	14	87	99	0.0602	0.0003	0.927	0.028	0.112	0.003	0.99	112	610	11	666	15	<b>683</b>	19
16	Millbay-feature124	58475	0.0	28	211	292	0.0569	0.0003	0.610	0.018	0.078	0.002	0.99	99	487	11	484	12	<b>483</b>	14
17	Millbay-feature139	233352	0.0	104	591	1137	0.0559	0.0002	0.609	0.018	0.079	0.002	0.99	109	450	9	483	12	<b>490</b>	14
18	Millbay-feature142	115474	0.0	45	36	524	0.0568	0.0002	0.663	0.020	0.085	0.003	0.99	108	483	9	516	12	<b>524</b>	15
19	Millbay-feature164	30801	0.1	14	95	126	0.0592	0.0003	0.766	0.023	0.094	0.003	0.99	101	573	11	577	13	<b>578</b>	17
19	Millbay-feature165	61683	0.0	26	93	230	0.0608	0.0003	0.863	0.026	0.103	0.003	0.99	100	631	9	632	14	<b>632</b>	18
20	Millbay-feature175	30990	0.1	14	108	156	0.0554	0.0003	0.582	0.018	0.076	0.002	0.99	110	430	11	466	11	<b>473</b>	14
21	Millbay-feature182	29606	0.1	14	108	111	0.0601	0.0003	0.847	0.026	0.102	0.003	0.99	104	606	11	623	14	<b>628</b>	18
22	Millbay-feature196*	44938	0.0	19	81	236	0.0540	0.0002	0.544	0.016	0.073	0.002	0.99	123	370	10	441	11	455	13
23	Millbay-feature198	13772	0.1	6	55	75	0.0573	0.0004	0.558	0.017	0.071	0.002	0.98	87	505	15	450	11	<b>439</b>	13
24	Millbay-feature224*	9441	0.2	5	65	52	0.0522	0.0004	0.500	0.016	0.069	0.002	0.96	148	293	19	411	10	433	13
25	Millbay-feature229	39449	0.0	17	31	76	0.0831	0.0004	2.292	0.069	0.200	0.006	0.99	92	<b>1272</b>	9	1210	21	1175	32
26	Millbay-feature241	174971	0.0	80	139	247	0.0921	0.0004	3.460	0.104	0.273	0.008	0.99	106	<b>1469</b>	7	1518	23	1554	41
27	Millbay-feature244*	19238	0.1	9	78	104	0.0530	0.0003	0.523	0.016	0.072	0.002	0.98	136	327	14	427	11	446	13
28	Millbay-feature250	31231	0.1	15	36	45	0.0939	0.0004	3.488	0.105	0.269	0.008	0.99	102	<b>1507</b>	9	1524	24	1537	41

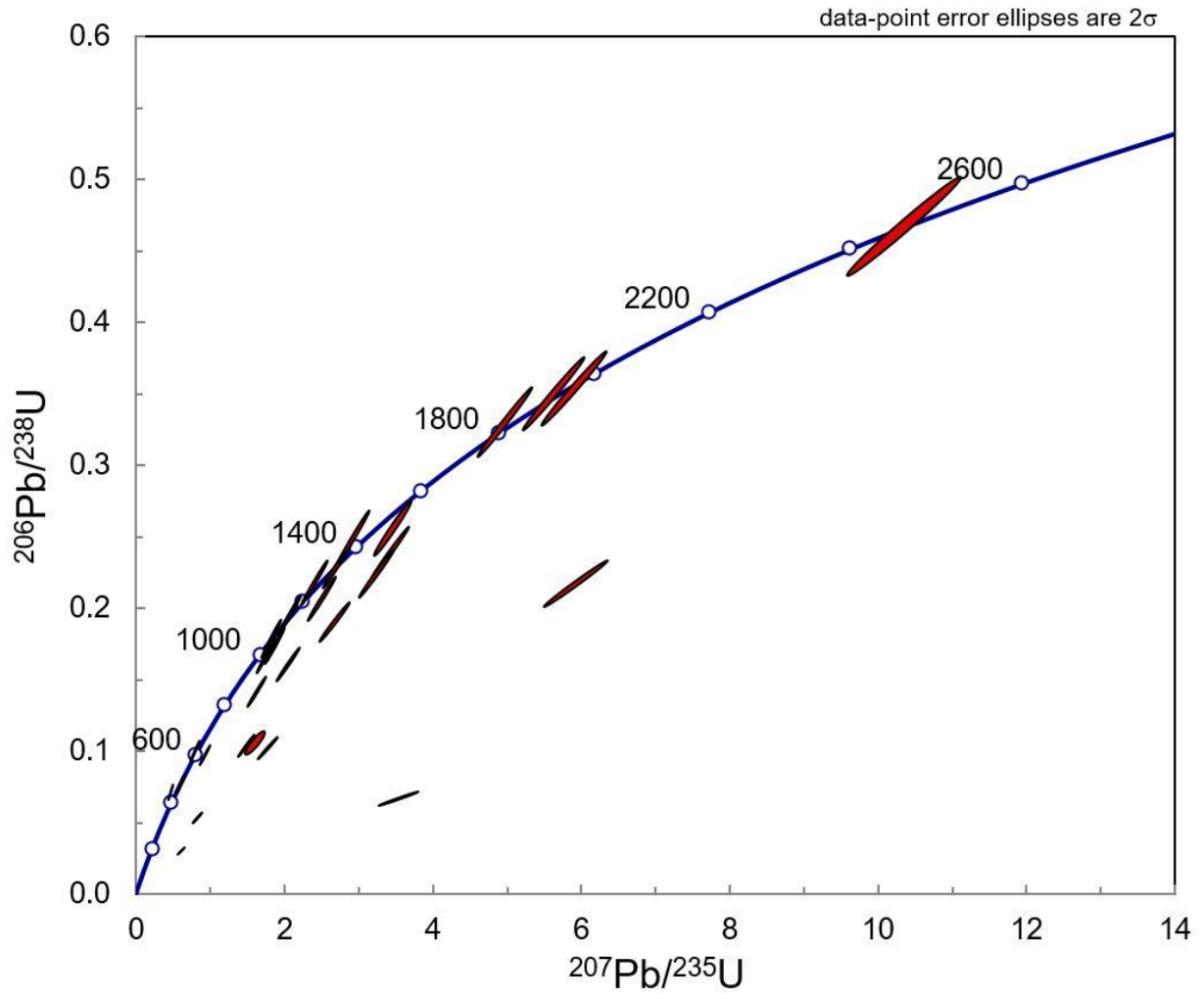
Data indicated by \* have high common Pb or are >15% discordant and therefore do not give reliable ages

Ages in bold represent preferred ages ( $^{207}\text{Pb}/^{206}\text{Pb}$  ages > 1Ga;  $^{238}\text{U}/^{206}\text{Pb}$  ages < 1 Ga)

$^{206}\text{Pb}_c$ (%) = percentage of common Pb

1s = 1 standard deviation of the data in the previous column

% concordance =  $^{238}\text{U} \cdot ^{206}\text{Pb}$  age /  $^{207}\text{Pb} \cdot ^{206}\text{Pb}$  age x 100



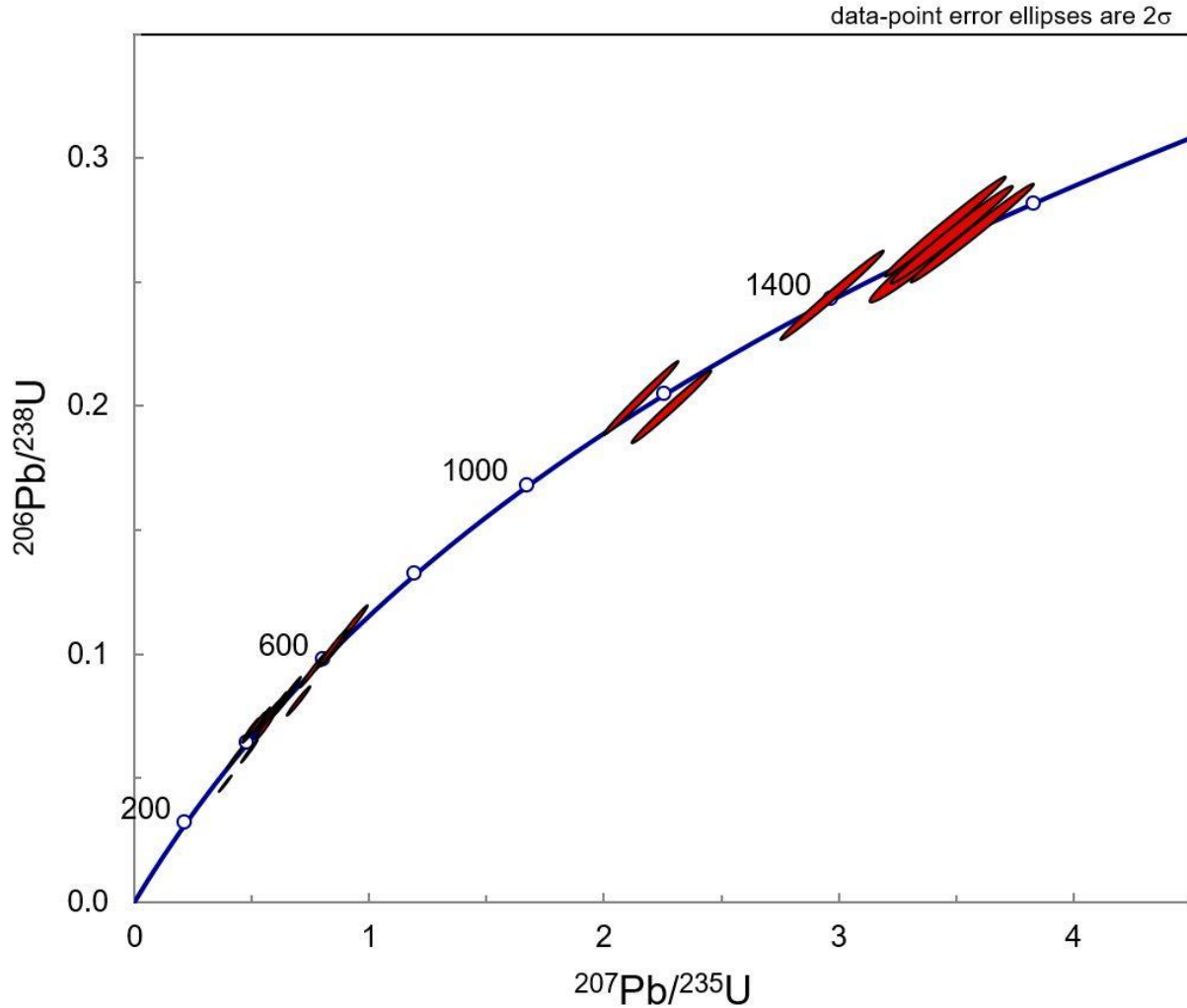
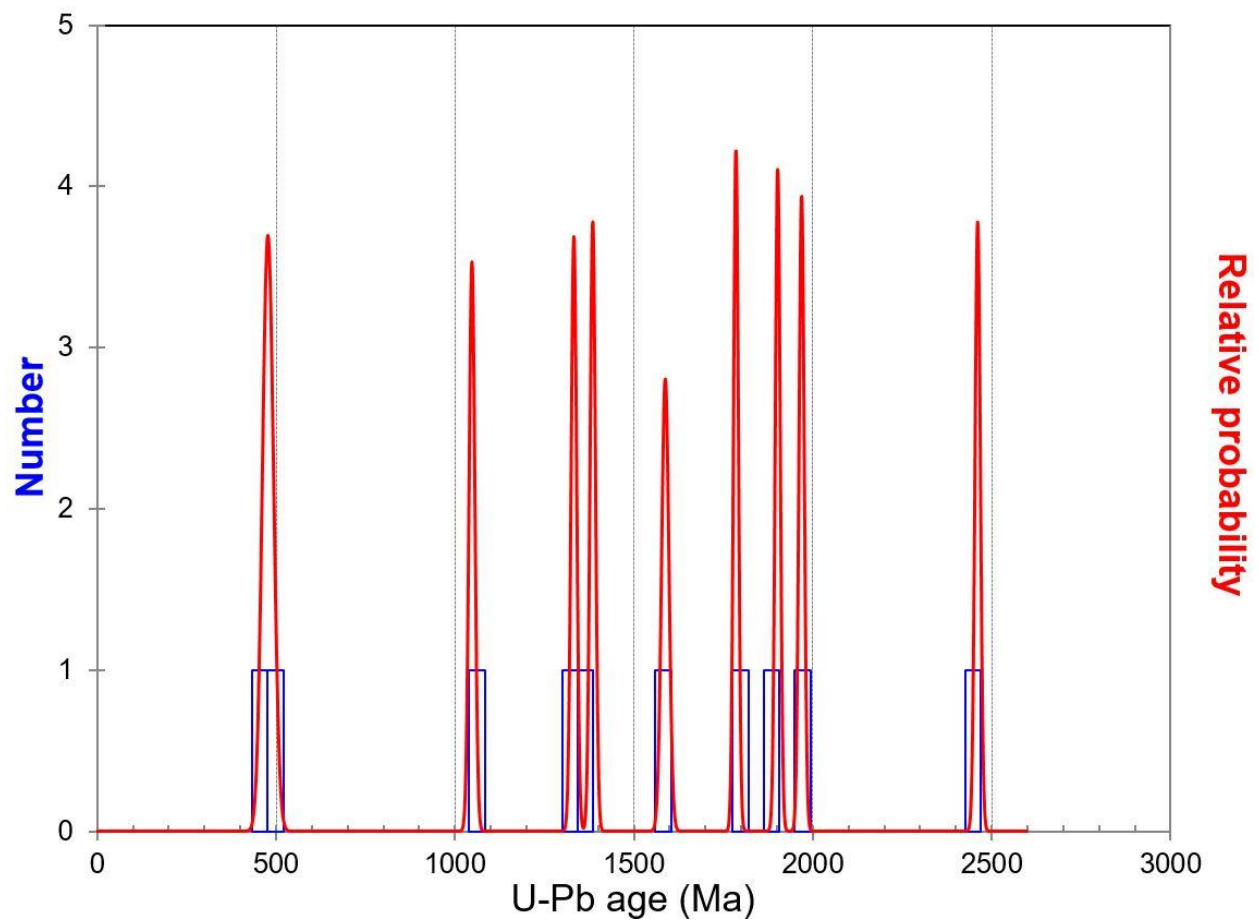


Fig. 7. Concordia diagrams for zircon grains measured in situ by LA-SC-ICPMS (a. upper is Altar Stone sample; b. lower is Cosheston Subgroup sample). Concordia is the curve connecting equal ages for two chronometers,  $\text{U}^{235}$  decaying to  $^{207}\text{Pb}$  and  $\text{U}^{238}$  decaying to  $^{206}\text{Pb}$ , which are running at very different rates. Grains plotting below Concordia have suffered radiogenic Pb loss and most of these have significant common Pb. Note the difference in scales in the two panels.



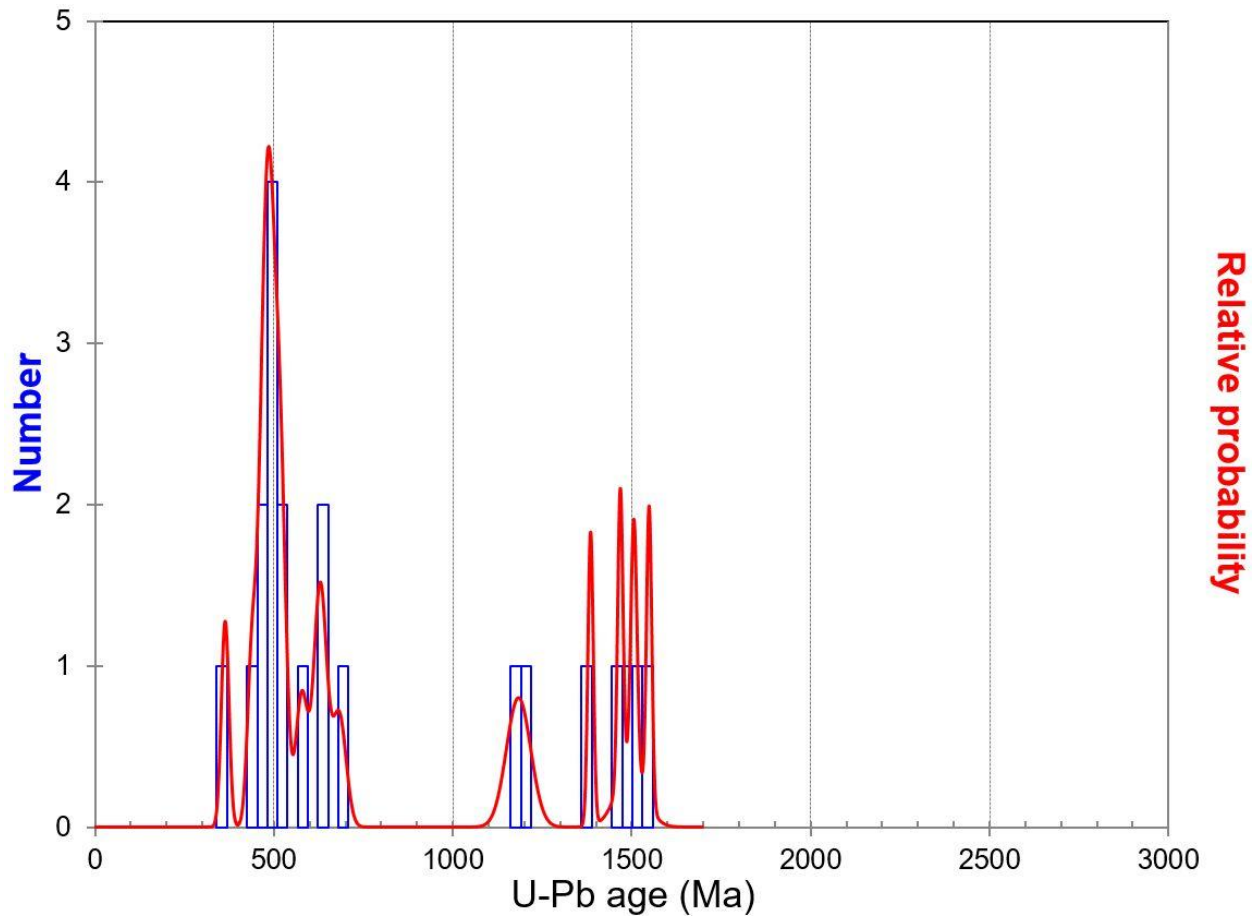


Fig. 8. U-Pb age probability density diagrams for the two samples analysed in this study (a. upper is Altar Stone sample; b. lower is Cosheston Subgroup sample). The age distribution of the grains is distinct for each sample (see text for discussion).

## 6. Discussion

Analysis using automated SEM-EDS has provided quantitative data which both supports but also modifies earlier petrographic observations to show that there are two different sandstones in the Stonehenge bluestone assemblage, namely the Lower Palaeozoic Sandstone of Ixer et al. (2017) and the Altar Stone interpreted as derived from the Cosheston Subgroup (Late Silurian-Devonian Old Red Sandstone) (see Ixer et al., 2020). The data reveal key mineralogical differences between the two types of sandstone, in particular the notably higher modal % of calcite along with the presence of kaolinite and barite in the Altar Stone sandstone, the latter

being absent in the Lower Palaeozoic Sandstone. The contrasting modal % of kaolinite in the two sandstone types might relate to contrasting metamorphic grades which have affected the source areas; kaolinite is typically present in diagenetic grade rocks (see Merriman and Frey, 1999), reacting to other minerals in anchizone and epizone rocks. Accordingly, the Lower Palaeozoic Sandstone is likely to be sourced from an area which shows a higher metamorphic grade than the source area for the Altar Stone. This is corroborated by textural evidence for the two sandstone types; the Lower Palaeozoic Sandstone shows a marked spaced cleavage whilst the Altar Stone sandstone shows little evidence for deformation, only showing a poorly developed planar fabric which is thought to be part depositional and part compactional in origin.

As detailed earlier in this paper, the Altar Stone has previously been linked to a source in the Cosheston Subgroup at Milford Haven, in west Wales. However, both the automated SEM-EDS data and the observations on the zircon populations and the U-Pb age dates obtained from zircons in the two types of sandstone provide quantitative evidence that the Altar Stone is not sourced from the Cosheston Subgroup at Mill Bay, which corroborates previous qualitative evidence from petrographic accounts (Ixer et al., 2020).

Comparing the Altar Stone with the Cosheston Subgroup sandstones, a major difference between these two types of sandstones lies in the markedly higher modal % of calcite in the Altar Stone sandstone, and the markedly lower modal % of plagioclase in the Altar Stone compared to the Cosheston Subgroup samples. In addition, the modal % of kaolinite is considerably lower in the Cosheston Subgroup samples compared to the Altar Stone sandstone, and barite is present throughout all of the Altar Stone samples but rare to absent (<0.01%) in the Cosheston Subgroup sandstones. Overall, the Cosheston Subgroup sandstones are higher metamorphic grade rocks than the Altar Stone sandstone.

One of the principal aims of this study was to determine the potential value of automated mineralogy in archaeological provenancing investigations. We have demonstrated that the technique convincingly determines that the two types of sandstone found at Stonehenge, the so-called Altar Stone sandstone and a sandstone of Lower Palaeozoic age, have different and discriminatory mineralogies and that neither sandstone type matches Cosheston Subgroup sandstone from Mill Bay, in west Wales, a previously proposed source for the Altar Stone. The



technique is especially useful when combined with complimentary techniques, in this case U-Pb age dating of zircons, which supports the discrimination of the Altar Stone and the Cosheston Group sandstone analysed samples.

Hillier et al. (2006) investigated the clay mineralogy of Old Red Sandstone rocks from an area covering south Wales, the Welsh Borderland and the West Midlands of England using X-ray diffraction. They concluded that in these rocks the metamorphic grade increases from east to west across this region. In particular whilst kaolinite is present in the east (eastern Wales, the Welsh Borderland and the West Midlands) it is not present in the west. This suggests that the Altar Stone sandstone is more likely to have been sourced in the eastern part of the area investigated by Hillier et al. (2006).

Interestingly, although H.H. Thomas (1923) had considered possible sources for the Altar Stone in the Milford Haven area (noting both Mill Bay and Llangwm) he also suggested that the 'Senni Beds' also offered a possible provenance, a contention later supported by R.G. Thomas (1991) and Ixer and Turner (2006). The Senni Formation crops out across south Wales, from Kidwelly in the west to the Crickhowell/Abergavenny area in the east, before the outcrop strikes more north-south along the eastern margin of the South Wales Coalfield syncline. Thus it is probable that the Altar Stone has a source considerably further east than Milford Haven (see Fig. 1).

From these results we conclude that the Altar Stone was not derived from the Mill Bay area in west Wales; a source further east, towards the English Border is considered more likely. This conclusion undermines the notion that the Stonehenge bluestones were transported by sea for a part of their transport to Stonehenge and reinforces the proposal by Parker Pearson et al. (2015a, 2019) that a land route is more likely following discovery of sources of rhyolitic and doleritic bluestones from the northern side of the Mynydd Preseli.

In order to investigate further the possible source of the Altar Stone a detailed XRD study of the clay mineralogy of the Altar Stone sandstone has been initiated in order to compare the clay mineral assemblage present with those in the comprehensive account by Hillier et al. (2006) to test whether the three types of sandstone under investigation show contrasting metamorphic grades and indicate broad source areas across south Wales.

Perhaps consideration should be given to a potential source for the Altar Stone from other areas in Britain, rather than being constrained by a source in Wales. Old Red Sandstone facies strata crop out widely across Britain, including the Welsh Borderland as far north as Shropshire, southern Scotland (in particular in the Midland Valley) and the Orcadian Basin in the Highlands and Islands and Grampian regions of northern Scotland.

Yet there are good reasons for considering that the Altar Stone may have derived from the eastern part of the Senni Formation in the Crickhowell/Abergavenny area since many standing stones are recorded in that part of south Wales. A close comparison in size and shape is the Growing Stone (also known as Cwrt y Gollen), a 4m-tall sandstone monolith beside the A40 road between Crickhowell and Abergavenny (Barber, 2017).

This eastern section of the Senni Formation lies on a natural routeway leading from west Wales to the Severn estuary and beyond. Followed today by the A40, its route along the valleys may well have been significant in prehistory, raising the possibility that the Altar Stone was added *en route* to the assemblage of Preseli bluestones taken to Stonehenge around or shortly before 3000 BC (Parker Pearson et al., 2019). Strontium isotope analysis of human and animal bones from Stonehenge, dating to the beginning of its first construction stage around 3000 BC, has revealed that four individuals and a cow have isotopic ratios consistent with having lived in this western region of Britain (Snoeck et al., 2018; Evans et al., 2019).

## **7. Conclusions**

What this study has clearly demonstrated, on the basis of quantitative data, is that the Cosheston Subgroup, exposed along Milford Haven in west Wales, is not the source of the Altar Stone, a conclusion reached previously on qualitative grounds by Thomas (1991), Ixer and Turner (2006) and Ixer et al. (2019, 2020). This interpretation removes the provenance-based grounds for the previously proposed sea route hypothesis for the transport of the Stonehenge bluestones from Milford Haven up the Bristol Channel, before transport along the River Avon and a final land transfer to Stonehenge. This accords with the identification of two bluestone quarries on the northern flanks of the Mynydd Preseli, at Craig Rhos-y-Felin and Carn Goedog (see Parker Pearson

et al., 2015a; 2019) which, because of their particular locations, have been considered to support transport of the bluestones to Stonehenge following a land route.

Acknowledging that the Altar Stone is most likely sourced at some considerable distance from the Mynydd Preseli (perhaps in excess of 150 km) it is reasonable to assume that there is no link between the Altar Stone and the bluestones which are known to have been sourced in the Mynydd Preseli area (the spotted and unspotted dolerites, the rhyolite from Craig Rhos-y-Felin and in all likelihood the other dacites/rhyolites and tuffaceous rocks), other than that the Altar Stone may have been collected *en route* from Preseli to Stonehenge and that they were all at some stage transported to and erected at Stonehenge. Thomas (1923) considered that all the bluestones (except for the Altar Stone) were all derived from a very restricted area and might have been erected originally as a 'venerated stone circle' at the eastern end of the Mynydd Preseli.

Finally, although automated mineralogy has been used in the study of archaeological ceramics (e.g. Knappett et al., 2011), cosmetics (e.g. Hardy et al., 2006) and in using soil forensics to test artefact provenancing (Pirrie et al., 2014) this study appears to be first application of automated mineralogy in the analysis of archaeological lithic material. Our findings highlight the potential value of the application of this technique in such studies, especially in combination with a complimentary technique such as LA-ICPMS single crystal U-Pb age dating.

### **Acknowledgements**

SGS Canada Inc. is acknowledged for providing automated SEM-EDS analysis time. Two anonymous reviewers provided valuable comments which greatly improved this contribution. We thank Brian John for collecting the Cosheston Subgroup samples and making them available for analysis.

### **Funding**

The University of South Wales is acknowledged for funding support through a CES RIS research grant. Zircon dating was supported through a research grant from Helford Geoscience LLP to the

University of Exeter. Amgueddfa Cymru-National Museum Wales funded fieldwork costs involved with this study.

## References

Armitage, P.J., Worden, R.H., Faulkner, D.R., Aplin, A.C., Butcher, A.R., Iliffe, J., 2010. Diagenetic and sedimentary controls on porosity in Lower Carboniferous fine-grained lithologies, Krechba field, Algeria: A petrological study of a caprock to a carbon capture site. *Marine and Petroleum Geology* 27, 1395-1410.

Atkinson, R.J.C., 1956. Stonehenge. Hamish Hamilton.

Barber, C., 2017. *Megaliths of Wales: mysterious sites in the landscape*. Amberley.

Bevins, R.E., Ixer, R.A., 2018. Retracing the footsteps of H.H. Thomas: a review of his Stonehenge bluestone provenancing study. *Antiquity* 363, 788-802.

Bevins, R.E., Atkinson, N., Ixer, R., Evans, J., 2017. U-Pb zircon age constraints for the Ordovician Fishguard Volcanic Group and further evidence for the provenance of the Stonehenge bluestones. *Journal of the Geological Society of London* 174, 14-17.

Bevins, R.E., Ixer, R.A., Pearce, N.P.G., 2014. Carn Goedog is the likely major source of Stonehenge doleritic bluestones: evidence based on compatible element geochemistry and Principal Component Analysis. *Journal of Archaeological Science* 42, 179-193.

Bevins, R.E., Ixer, R. A., Webb, P.C., Watson, J.S., 2012. Provenancing the rhyolitic and dacitic components of the Stonehenge landscape bluestone lithology: new petrographical and geochemical evidence. *Journal of Archaeological Science* 39, 1005-1019.

Bevins, R.E., Pearce, N.J.G., Ixer, R.A., 2011. Stonehenge rhyolitic bluestone sources and the application of zircon chemistry as a new tool for provenancing rhyolitic lithics. *Journal of Archaeological Science* 38, 605-622.

Carter, A., Riley, T.R., Hillenbrand, C.-D., Rittner, M., 2017. Widespread Antarctic glaciation during the late Eocene. *Earth and Planetary Science Letters* 458, 49-57.

Cleal, R.M.J., Walker, K.E., Montague, R., 1995. *Stonehenge in its landscape*. English Heritage. 618pp.

Darvill, T., 2006. *Stonehenge: The Biography of a Landscape*. Tempus Publishing Ltd, Stroud, 319pp.

Darvill, T., Wainwright, G., 2009. Stonehenge excavations 2008. *Antiquaries Journal* 89, 1-19.

Evans, J., Parker Pearson, M., Madgwick, R., Sloane, H. & Albarella, U., 2019. Strontium and oxygen isotope evidence for the origin and movement of cattle at Late Neolithic Durrington Walls, UK. *Archaeological and Anthropological Sciences* 11, 5181–5197. <https://doi.org/10.1007/s12520-019-00849-w>

Hardy, A.D., Walton, R.I., Vaishnav, R., Myers, K.A., Power, M.R. & Pirrie, D., 2006. Egyptian eye cosmetics ('kohl's'): past and present. In: Bradley, D. & Creagh, D. (eds) *Physical techniques in the study of art, archaeology and cultural heritage*. Elsevier, 173-203.

Hilditch, J., Pirrie, D., Knappett, C., Rollinson, G.K. & Momigliano, N., 2016. Taking the rough with the smooth: using automated SEM-EDS to integrate coarse and fine ceramic assemblages in the Bronze Age Aegean. In: *Sibbesson, E., Jervis, B. & Coxon, S. (eds), Insights from innovation: new light on archaeological ceramics*, Highfield Press, 74-96.

Hillier, S., Wilson, J., Merriman, R.J., 2006. Clay mineralogy of the Old Red Sandstone and Devonian sedimentary rocks of Wales. *Clay Minerals* 41, 433-471.

Horstwood M.S.A., Kosler J., Gehrels G. et al., 2016. Community-Derived Standards for LA-ICP-MS U-(Th)-Pb Geochronology - Uncertainty Propagation, Age Interpretation and Data Reporting. *Geostandards and Geoanalytical Research* 40, 311-332. DOI: 10.1111/j.1751-908X.2016.00379.x

Howard, H., 1982. A petrological study of the rock specimens from excavations at Stonehenge, 1979-80 in M.W. Pitts (ed.), *On the road to Stonehenge: reports on investigations beside the A344 in 1968, 1979 and 1980*. *Proceedings of the Prehistoric Society* 48, 104-126.

Huhma, H., Mänttari, I., Peltonen, P., Kontinen, A., Halkoaho, T., Hanski, E., Hokkanen, T., Hölttä, P., Juopperi, H., Konnunaho, J., Layahe, Y., Luukkonen, E., Pietikäinen, K., Pulkkinen, A., Sorjonen-Ward, P., Vaasjoki, M., Whitehouse, M., 2012. The age of the Archaean greenstone belts in Finland. *Geological Survey of Finland, Special Paper* 54, 74-175.

Hunt, A.M.W., (Ed.) 2016. *The Oxford handbook of archaeological ceramic analysis*. Oxford: Oxford University Press.

Ixer, R.A., Bevins, R.E., 2010. The petrography, affinity and provenance of lithics from the Cursus Field, Stonehenge. *Wiltshire Archaeological & Natural History Magazine* 103, 1-15.

Ixer, R.A., Bevins, R.E., 2011a. Craig Rhos-y-felin, Pont Saeson is the dominant source of the Stonehenge rhyolitic debitage. *Archaeology in Wales* 50, 21-31.

Ixer, R.A., Bevins, R.E., 2011b. The detailed petrography of six orthostats from the Bluestone Circle, Stonehenge. *Wiltshire Archaeological & Natural History Magazine* 104, 1-14.

Ixer, R.A., Bevins, R.E., 2013. Chips off the old block The Stonehenge debitage dilemma. *Archaeology in Wales* 52, 11-22.

Ixer, R.E., Bevins, R.E., 2016. Volcanic Group A debitage: its description and distribution within the Stonehenge Landscape. *Wiltshire Archaeological & Natural History Magazine* 109, 1-14.

Ixer, R.A., Turner, P., 2006. A detailed re-examination of the petrography of the Altar Stone and other non-sarsen sandstones from Stonehenge as a guide to their provenance. *Wiltshire Archaeology and Natural History Magazine* 99, 1-9.

Ixer, R.A., Bevins, R.E., Gize, A.P., 2015. Hard 'Volcanics with sub-planar texture' in the Stonehenge landscape. *Wiltshire Archaeological & Natural History Magazine* 108, 1-14.

Ixer, R.A., Bevins, R.E., Pirrie, D., Turner, P., Power, M., 2020. 'No provenance is better than wrong provenance': Milford Haven and the Stonehenge sandstones. *Wiltshire Archaeology and Natural History Magazine* 113, 1-15.

Ixer, R.A., Bevins, R.E., Turner, P., Power, M., Pirrie, D., 2019. Alternative Altar Stones? Carbonate-cemented micaceous sandstones from the Stonehenge Landscape. *Wiltshire Archaeology and Natural History Magazine* 112, 1-13.

Ixer, R.A., Turner, P., Molyneux, S., Bevins, R.E., 2017. The petrography, geological age and distribution of the Lower Palaeozoic Sandstone debitage from the Stonehenge Landscape. *Wiltshire Archaeology and Natural History Magazine* 110, 1-16.

John, B., Elis-Gruffydd, D., Downes, J., 2015. Quaternary events at Craig Rhosyfelin, Pembrokeshire. *Quaternary Newsletter* October 2015 (No 137), 219-232.

Knappett, C., Pirrie, D., Power, M.R., Nikolakopoulou, I., Hilditch, J., Rollinson, G.K., 2011. Mineralogical analysis and provenancing of ancient ceramics using automated SEM-EDS analysis (QEMSCAN®): a pilot study on LB I pottery from Akrotiri, Thera. *Journal of Archaeological Science* 38, 219-232.

Ludwig, K.R., 2003. User's manual for Isoplot/Ex, Version 3.00. A geochronological toolkit for Microsoft Excel. Berkeley Geochronology Center Special Publication No.4.

Merriman, R.J., Frey, M., 1999. Patterns of very low-grade metamorphism in metapelitic rocks. In: Frey, M, Robinson, D. (eds). *Low-Grade Metamorphism*. Blackwells, Oxford, 61-107.

Müller, W., Shelley, M., Miller, P., Broude, S., 2009. Initial performance metrics of a new custom-designed ArF excimer LA-ICPMS system coupled to a two-volume laser-ablation cell." *Journal of Analytical Atomic Spectrometry* 24, 209-214.

Parker Pearson, M., 2016. The sarsen stones of Stonehenge. *Proceedings of the Geologists' Association* 127, 363-369.

Parker Pearson, M., Bevins, R.E., Ixer, R.A., Pollard, J., Richards, C., Welham, K., Chan, B., Edinborough, K., Hamilton, D., McPhail, R., Schlee, D., Schwenninger, J-L., Simmons, E., Smith, M., 2015a. Craig Rhos-y-felin: a Welsh bluestone megalith quarry for Stonehenge. *Antiquity* 89, 1331-1352.

Parker Pearson, M., Pollard, J., Richards, C., Thomas, J., Welham, K., 2015b. Stonehenge: making sense of a prehistoric mystery. Council for British Archaeology, 120pp.

Parker Pearson, M., Pollard, J., Richards, C., Welham, K., Caswell, C., French, C.A.I., Shaw, D., Simmons, E., Stanford, A., Bevins, R.E., Ixer, R.A., 2019. Megalithic quarries for Stonehenge's bluestones. *Antiquity* 93, 45-62.

Pirrie, D., Rollinson, G.K., 2011. Unlocking the application of automated mineralogy. *Geology Today* 27, 226-235.

Pirrie, D., Butcher, A.R., Power, M.R., Gottlieb, P., Miller, G.L., 2004. Rapid quantitative mineral and phase analysis using automated scanning electron microscopy (QEMSCAN); potential applications in forensic geoscience. In K. Pye and D. Croft (eds). Geological Society, London, Special Publication 232, 123-136.

Pirrie, D., Rollinson, G.K., Andersen, J.A., Wootton, D. & Moorhead, S., 2014. Soil forensics as a tool to test reported artefact find sites. *Journal of Archaeological Science* 41, 461-473.

Pirrie, D., Rollinson, G.K., Power, M.R., Webb, J., 2013. Automated forensic soil mineral analysis; testing the potential of lithotyping. In D. Pirrie, A. Ruffell and L.A. Dawson (eds). *Environmental and criminal geoforensics*. Geological Society of London, Special Publication 384, 47-64.

Snoeck, C., Pouncett, J., Claeys, P., Goderis, S., Mattielli, N., Parker Pearson, M., Willis, C., Zazzo, A., Lee-Thorp, J. and Schulting, R., 2018. Strontium isotope analyses on cremated human remains from Stonehenge support links with west Wales. *Scientific Reports* 8, 10790.

Stacey, J.S., Kramers, J.D., 1975. Approximation of terrestrial lead isotope evolution by a two-stage model. *Earth and Planetary Science Letters* 26, 207-221.

Strahan, A., Cantrill, T.C., Dixon, E.E.L., Thomas, H.H., Jones, O.T., 1914. Geology of the South Wales Coalfield, Part XI, The country around Haverfordwest. *Memoir of the Geological Survey of Great Britain*. London: HMSO.

Thomas, H.H., 1923. The source of the stones of Stonehenge. *The Antiquaries Journal* 3, 239-60.

Thomas, R.G., 1991. Petrography and possible provenance of sandstone sample OU9 (Aubrey Hole 1) and a comment on the Altar Stone. Appendix 2 in R.S. Thorpe, O. Williams-Thorpe, D.G. Jenkins and J.S. Watson (eds). *The Geological Sources and Transport of the Bluestones of Stonehenge, Wiltshire, UK*. *Proceedings of the Prehistoric Society* 57, 152-3.

Thorpe, R.S., Williams-Thorpe, O., Jenkins, D.G., Watson, J.S. with contributions by R.A. Ixer and R.G. Thomas, 1991. *The Geological Sources and Transport of the Bluestones of Stonehenge, Wiltshire, UK*. *Proceedings of the Prehistoric Society* 57, 103-157.

Van Achterbergh, E., Ryan C., Jackson, S., Griffin W., 2001. Data reduction software for LA-ICP-MS, in: *Laser-Ablation ICPMS in the Earth Sciences – Principles and applications*, Mineralogical Association of Canada short course series, 29, St. John's, Newfoundland, Sylvester, P. (Ed.), 239-243.